

Process variations of a Neoproterozoic delta system in response to the influence of mixed-energy systems and sea-level fluctuation: an insight from Simla Group, Lesser Himalaya, India

Priyanka Mazumdar¹, Ananya Mukhopadhyay^{1,*}, Tithi Banerjee¹, Alono Thorie¹,
Patrick G Eriksson²

¹ Department of Earth Sciences, Indian Institute of Engineering Science & Technology, Shibpur, Howrah, West Bengal 711103, India

² Department of Geology, University of Pretoria, Pretoria, South Africa

*Correspondence to: Ananya Mukhopadhyay. Email: ananyageol@gmail.com

Abstract

Deltas generally exhibit morphological and architectural variations due to repercussions of fluvial, wave and tidal currents. The Neoproterozoic Chhaosa Formation, Simla Group, Lesser Himalaya, a shallow-marine, mixed-energy deltaic system represents a unique example of variability of those processes at different scales. Outcrop-based facies analysis was combined with application of sequence stratigraphy in the present study to elucidate signatures of fluvial, tide and wave currents. The proximal part of the delta plain deposits (FA1) displaying fluvial attributes like sand sheets, large and small scale trough cross-beddings, channels, are combined with tidal activity. Delta front (FA2) deposits and prodelta deposits (FA3) essentially record mixed tidal and wave activity like mud drapes, flasers, lenticular, wavy beddings, syneresis cracks, tidal rhythmites, low angle cross-stratification oscillation ripples, hummocky and swaley cross-stratifications. Coastal process classification ternary plots are prepared to identify the interplay of different processes and their control in the deposition of Chhaosa delta system. The Chhaosa Formation has developed during elevated pulse rates of progradation and retrogradation, overlapped with elongated phases of progradation. A comparison between the Chhaosa delta and modern as well as ancient delta system has been made to understand the control of mixed-energy processes on sedimentation patterns throughout the global history.

Keywords: Mixed-energy delta; Neoproterozoic Chhaosa Formation; Simla Group; Retrogradation; Progradation; Coastal process classification ternary plots

Introduction

Deltas have been broadly categorized according to the dominance of fluvial, wave and tidal energy. A study on numerous deltas reveals that the deltas generally reflect the synergy of fluvial, tidal and wave mechanisms (Brown Jr et al. 1990; 1973; Olariu et al. 2010; Vakarelov et al. 2012; Eide et al. 2016; Peng et al. 2018). Evaluation of mixed-energy deltas encompasses a coeval composite of fluvial, wave and tidal energies. However, the intensity and preservation potential of every system varies through space and time (Ta et al. 2002a,

b; Dalrymple et al. 2003; Ainsworth et al. 2011; Rossi and Steel 2016). Hence, it is essential to recognize and differentiate the evidence of the three predominant processes (fluvial, tides and waves) by the application of outcrop-based facies analysis. Facies analysis revealed that the Chhaosa Formation represents a unique case history of a mixed-energy system with diverse processes.

Sedimentological analysis of the Chhaosa Formation exhibits the contrasts between mixed-energy delta systems from standard river, tide, or wave-dominated deltas. Objectives of this work are: (i) to interpret different lithofacies and facies associations; (ii) to enumerate the features of river, tide and wave currents; (iii) to analyse the controls and effects of mixed-energy processes in the Neoproterozoic Chhaosa deltaic system by preparing coastal process classification ternary plots based on sand–shale ratios, sand–body geometries and various sedimentary structures deposited by various processes; (iv) a comparison between the inferred Chhaosa delta system and other delta systems has been elucidated to understand the control of mixed-energy system in ancient as well as in the modern coastal systems.

Geological framework

Constituting an essential stratigraphic element of the Lesser Himalayas of India, Simla Group (Fig. 1) of rocks broadly comprises a coarsening upward clastic succession which was primarily recorded as the Infra-Blaini by Medlicott (1864). It unconformably overlies the Mesoproterozoic Shali Group and Neoproterozoic Darla volcanics (Table 1). It is broadly categorized into: Basantpur Formation, Kunihar Formation, Chhaosa Formation and Sanjauli Formation (Geological Survey of India 1976). Sedimentation of the Shimla group of rocks started with the lowermost Basantpur Formation, which represents a carbonate ramp (Mukhopadhyay and Banerjee 2016), over which the Kunihar Formation was laid down in a tidally influenced shallow marine environment (Mukhopadhyay and Thorie 2016; Thorie et al. 2018; Thorie et al. 2020). Chhaosa Formation has direct conformable contact with both Basantpur and Kunihar Formation. Significant evidence of deltaic environment has been observed from the intermediate sections of the Basantpur Formation which advanced into the Chhaosa Formation (Kumar and Brookfield 1987). With the gradual shallowing of the basin, Sanjauli Formation was deposited in a braided fluvial setting and marks the demise of Simla Basin (Mukhopadhyay et al. 2016). Studies on detrital micas and zircons of Simla Group have generated ages of 860 Ma and 770–850 Ma sequentially (Frank et al. 2001; McKenzie et al. 2011), furnishing that the Simla Group belongs to Neoproterozoic Era.

The current work encompasses a sedimentologic study of the deltaic Chhaosa Formation constituting a rhythmic sequence of sandstone, siltstones and shales with profuse development of flute, load casts and current ripples, flaser, lenticular, wavy beddings and mud drapes. The sandstones are predominantly medium to coarse-grained and tabular bedded marked with cross-, trough- and hummocky stratifications. Chhaosa shales are characteristically green or grey and occasionally purple in colour (Geological Survey of India 1976; Kumar and Brookfield 1987).

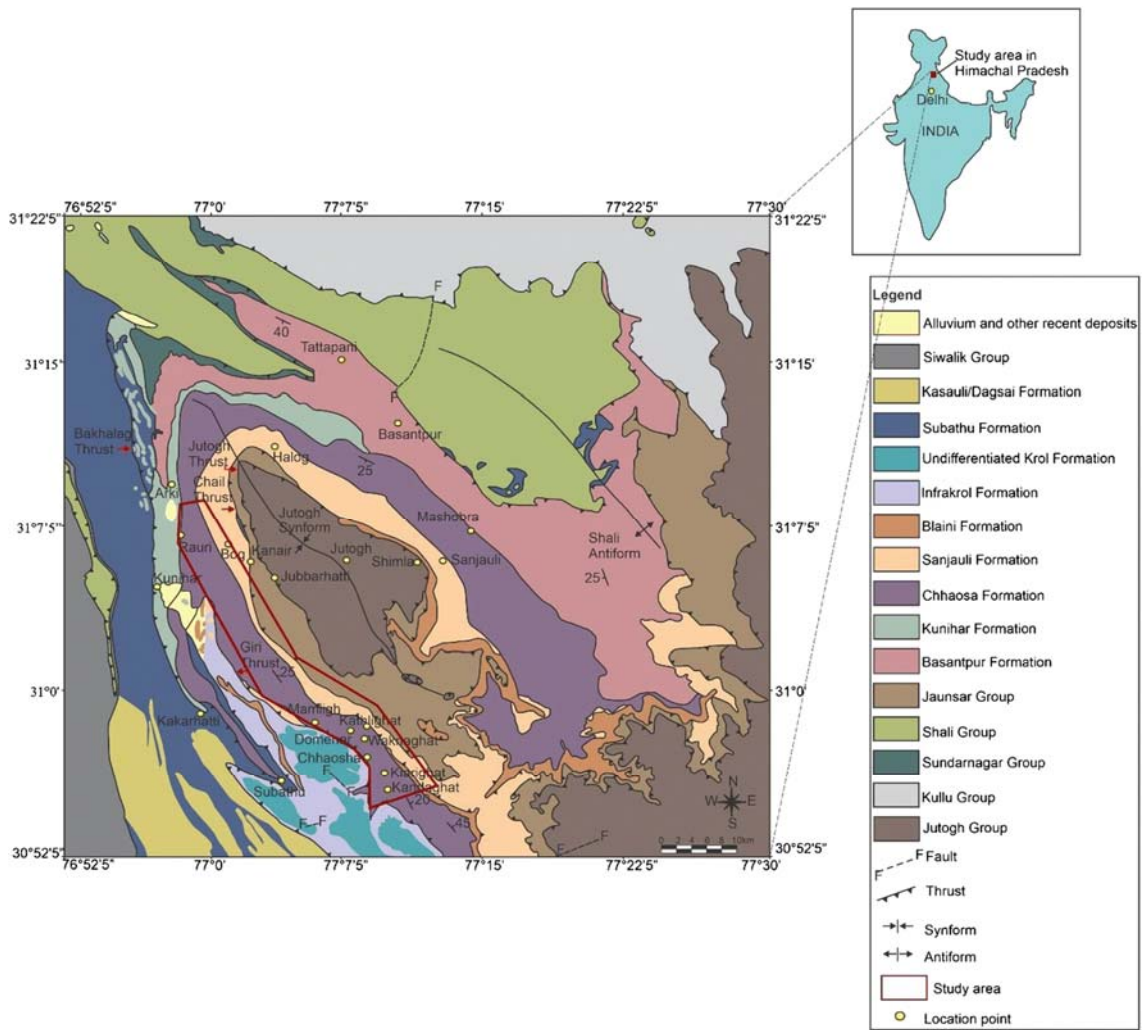
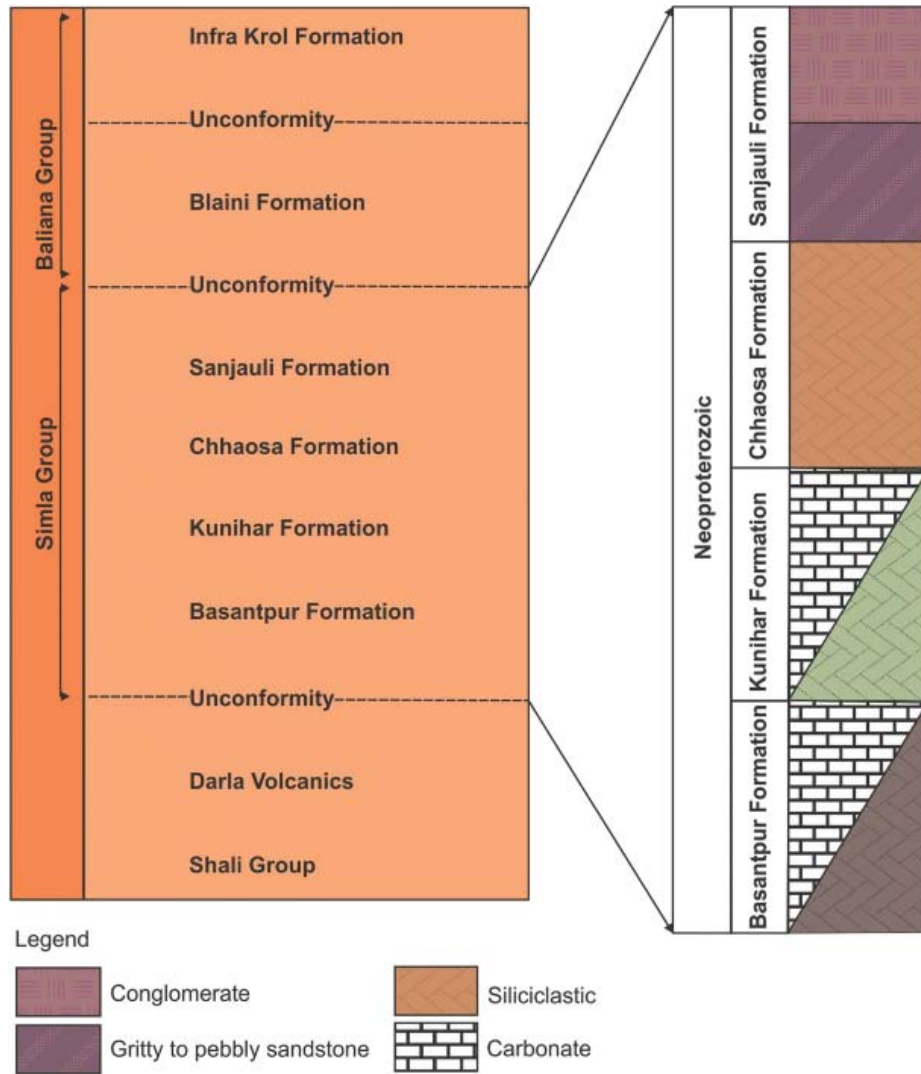


Fig. 1. Geological map of the Simla Group of rocks (modified after GSI, 1976). Red-coloured box demarcating the study area

Table 1 Generalised stratigraphy of the Simla Group (modified after GSI 1976)



Methods

Detailed field analysis of the study area was carried out to delineate various facies and their associations. This study involves the documentation of facies stacking pattern, primary sedimentary structures, thicknesses of beds, vertical lithologies, correlative panel and process dominance to delineate the vertical and spatial facies variabilities, and depositional environment. The field data has been supplemented with photographs. Maps were compiled from previously published articles and imageries from Google Earth Pro. Fifty rock thin sections have been prepared from collected rock samples to study the petrography. Based on sand–shale ratios, sand–body geometries and various sedimentary structures deposited by various processes (fluvial, wave and tide) a semi quantitative process-based ternary diagram (modified after Galloway 1975 and Ainsworth et al. 2011) has been made and plotted to identify the process variability throughout the chosen sections of the study area. The ternary diagram has been drawn by using AutoCad 2010.

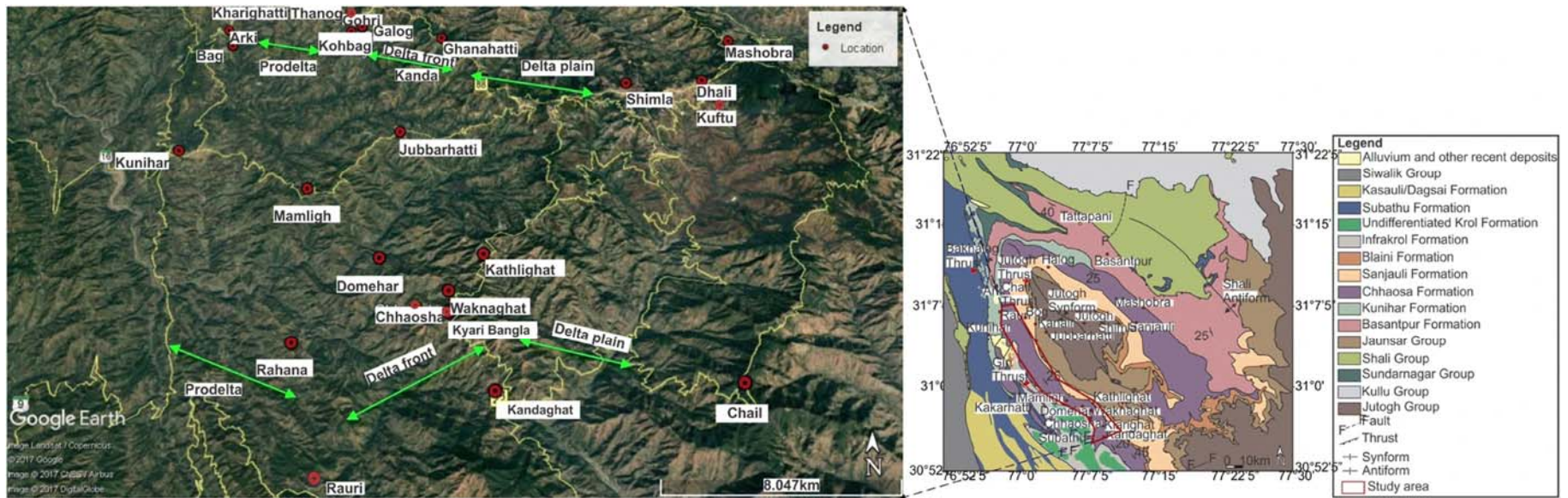


Fig. 2. Google Earth Pro image showing the location of the chosen sections of Chhaosa Formation (Fig. 1). Different parts of the Chhaosa delta system (delta plain –FA1, delta front –FA2, prodelta –FA3) are well exposed along the chosen transects in the study area

Facies description and interpretation

Outcrop-based facies analysis was carried out in the middle and upper segment of the Chhaosa Formation along Kandaghat–Kaithlighat, Kiarighat–Waknaghat, Domehar–Chhaosha, Kuftu–Rauri, Ghanahatti–Gohri, Kanda–Kannair, Khiari–Miaon, Dangi–Tudul, Bog–Arki, Rouri–Arki transects and in and around Baliana river section, Kohbag, Bog, Chayabag, Ukhru, Kothighati villages (Fig. 2). The Chhaosa Formation comprises sandstones, siltstones and silty-shales. The sandstones are generally medium- to fine-grained, moderately sorted but coarse-grained sandstones are also observed. Some of the sandstones are micaceous. Three major facies associations were identified: delta plain deposits (FA1), delta front deposits (FA2) and prodelta deposits (FA3) by analysing lithology, texture, grain size and internal sedimentary structure.

Delta plain deposits (FA1)

FA1 deposits are observed along Kandaghat–Waknaghat and Waknaghat–Domehar traverses (Fig. 2). The facies association consists of channelised erosionally-based sandstones (F1), thin-bedded siltstone and mud (F2). The rocks in FA1 are generally arenites. FA1 dominates the proximal part of the succession in the study area and interfingers with the delta front deposits (FA2).

Channelised erosionally-based sandstones (F1)

Description

Facies F1 represented by fining upward successions of buff-coloured coarse-grained concave-up erosionally scoured based sandstones (Fig. 3a, height varies from 12 to 18 cm width varies from 67 to 75 cm) are preserved along the Kandaghat–Waknaghat mountainous region for 7–8 km. Trough cross-stratified sandstone units are the most common occurrences in F1 which laterally pinch-out into 25 to 30 cm thick massive sandstone beds (lateral continuity of 50–55 m) in the lower interval. The troughs are generally 7–10 cm thick and laterally continuous for 26–38cm (Fig. 3b). Shallow channelized sandstones are coupled with ripple cross-laminations (thickness varies from 2 to 5 cm), in the upper intervals (Fig. 3c). Soft sediment deformation structures (ball and pillow structures) are present at lower intervals. Ball structures (Fig. 3d) are 14–15cm thick, 18–22 cm laterally extend and pillow structures are 10–12 cm thick and 20–25cm laterally extend. These erosive-based sand bodies cut into F2 deposits at places.

Interpretation

Profuse development of concave-up erosionally-based scour surfaces with fining upward successions indicated that F1 is deposited within distributary channels (Bhattacharya and Walker 1991; Gugliotta et al. 2016). The shape of channels, coarse size of grains and widespread trough cross-stratifications reflect channel deposits with dominant fluvial influence (Uroza and Steel 2008; Magalhães et al. 2015). Trough cross-stratifications result as a repercussion of two-dimensional and three-dimensional dune migrations (Skelly et al. 2003; Zieliński and Widera 2020). The channels with relatively shallower depth, associated



Fig. 3. Field photographs of channelised erosion-based sandstones (F1) of delta plain deposit (FA1) are observed along the Kandaghat–Kaithlighat traverse. **(a)** The base of the channel is marked by an erosional surface. Yellow arrow marks the base of channel. Scale: length of scale =6cm. **(b)** Trough cross-stratifications in F1. Yellow arrow shows the base of trough and black arrow marks the base of channel. Scale: length of hammer =32.5cm. **(c)** Ripple cross-laminations in coarse sandstone units. Red arrow indicates ripple cross-laminations. Scale: length of diagonal scale =15cm. **(d)** Profuse development of ball structures due to fluvial flooding. Scale: length of scale =5cm

with ripple cross-laminations are indicative of distributary channel deposition in a lower delta plain depositional setup (Rossi and Steel 2016). Ball and pillows are probably deposited by gravity loading in high hydrodynamic condition generated by fluvial flooding (Tanner and Lucas 2010; Zhang et al. 2018). F1 suggests delta-plain distributary channels where there is a decrease in fluvial energy in the direction of more distal environments.

Thin-bedded sandy siltstone and mud (F2)

Description

F2 is represented by fining-upward heterolithic successions of buff-coloured laminated sandy siltstones (12 to 15cm thick) intercalated with mudstone units (1 to 2 cm thick) which generally display a sheet-like geometry (Fig. 4a). Outcrops of F2 are found to be laterally extended along strike direction for about 5–6 km in and around Domehar village in the northwest of Kandaghat. The heteroliths of F2 mainly comprise plane-parallel laminations (0.4–0.6cm thick) (Fig. 4b) with small scale micro ripple laminations (0.5–0.9cm thick) (Fig. 4c). Heterolithic beddings (flaser, lenticular and wavy beddings) are common throughout the successions in F2 (Fig. 4d). The lower intervals of F2 are characterized by sandy siltstone units of 50–60 cm thickness with numerous scour surfaces whereas the upper intervals are dominated by 26 to 30 cm thick parallel-laminated mudstone units. Load structures such as flame (0.4–0.5cm thick), diaper structure (0.3–0.5cm thick) and complex structures (5–7cm thick) have been found at several units (Fig. 4d).

Interpretation

F2 is interpreted as an overbank counterpart of F1 (Fernández et al. 1988; Shukla et al. 2010; Buatois et al. 2012). The overall fining upward characteristics and tabular sheet-like geometry reflect channel overflow deposition during fluvial flooding over a large area (Spalletti and Piñol 2005; Hampton and Horton 2007; De Souza et al. 2019). Deposition of the finer silt reflects suspension due to gravity loading during low-energy sedimentation (Dasgupta 2005; Buatois et al. 2012; Kiwango and Mishra 2020). Continual changes in current velocities lead to the development of interbedded siltstone and mudstone deposits (Taral and Chakraborty 2018; Kiwango and Mishra 2020). The dominance of plane parallel laminations with ripple lamination represents a fluctuation in flow energy conditions, characterising hyperpycnal beds (Mulder et al. 2003; Olariu et al. 2010). The presence of heterolithic units (especially flaser, lenticular and wavy beddings) points towards the deposition of F2 in a lower delta plain environment by tidal currents (Jaiswal and Bhattacharya 2018). Extensive fining and thinning upward sandstone units with numerous scoured bases can be interpreted as channel deposits formed during high-energy fluvial flooding (Horne et al. 1978; Buatois et al. 2012). The presence of load and complex structures in the alternating sand–silt and clay layers indicates that these soft-sediment deposition structures probably deposited in a floodplain during fluvial surges (Rana et al. 2016; Shanmugam 2017).

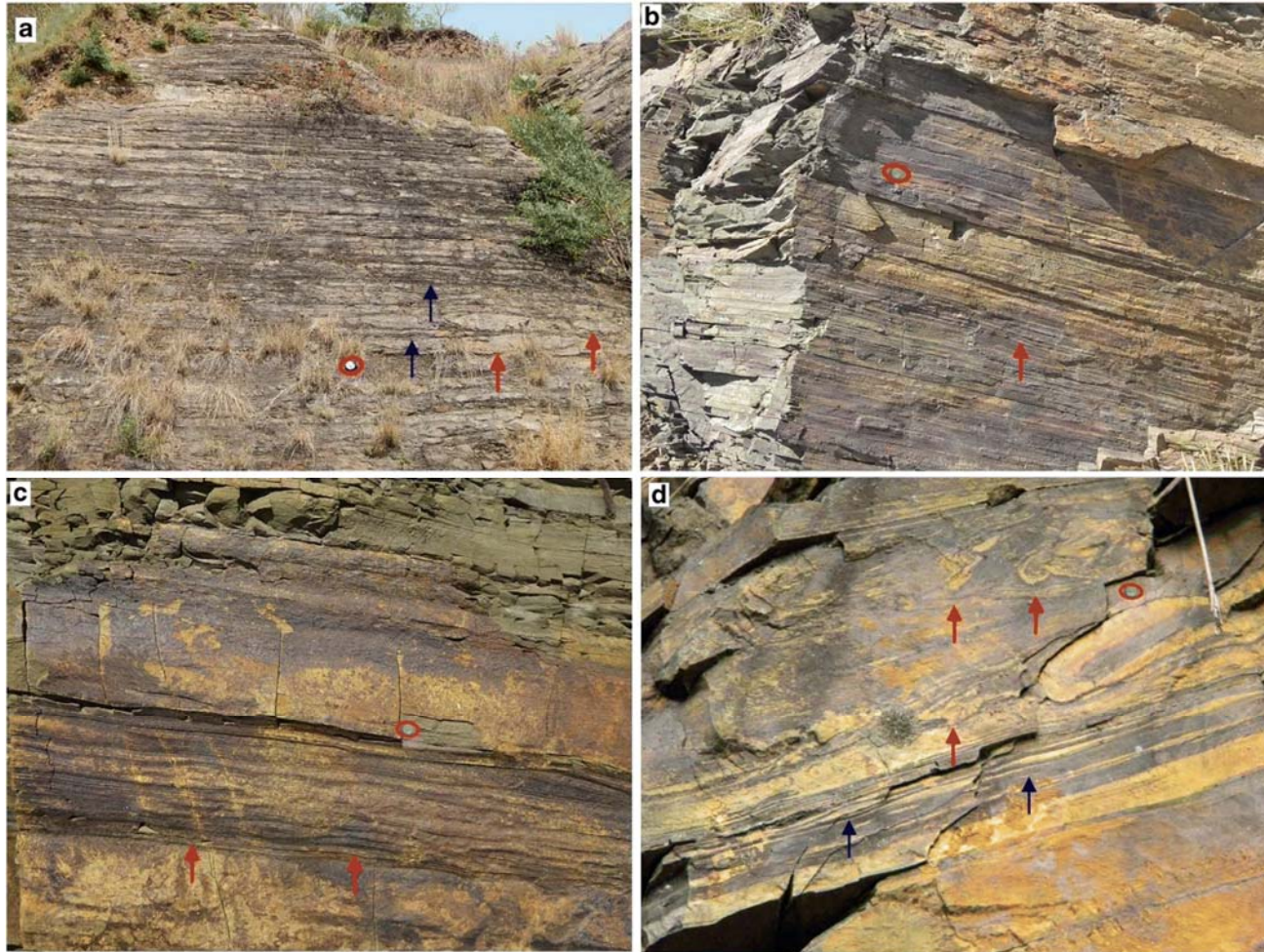


Fig. 4. Field photographs of thin-bedded sandy siltstone and mud (F2) of delta plain deposit (FA1) is observed in and around Wagnaghat village. **(a)** Laminated sandy siltstones intercalated with mudstone units displaying a sheet-like geometry. Red arrows indicate sandy silt units, and blue arrows mark the mud units. Scale: length of the clinometer = 9cm. **(b)** Heteroliths of F2 mainly comprise plane-parallel laminations. Red arrow indicates parallel laminations. Scale: diameter of coin =3cm. **(c)** Small scale ripple laminations are present. Red arrows indicating ripple laminations. Scale: diameter of coin =3cm. **(d)** Heteroliths of silt–mud representing lenticular bedding and complex structure. Blue arrows show lenticular beddings and red arrows mark complex structures. Scale: diameter of coin =3cm

Delta front deposits (FA2)

FA2 comprises depositional elements: (a) Proximal delta front (FA2a); (b) Distal delta front (FA2b). The facies association has been documented along Domehar–Chhaosha, Kuftu–Rauri, Ghanahatti–Gohri, Kanda–Kannair, Khiari–Miaon and Danggi–Tudul road sections (Fig. 2).

Proximal delta front (FA2a)

FA2a is composed of thick sandstone beds with thicknesses of about 3.5 m and a few hundred metres wide and is well observed along Domehar–Chhaosha, Kuftu–Rauri, Ghanahatti–Gohri and Kanda–Kannair road transects. The sand bodies show inverse grading from medium- to fine-grained sandstones, to succeeding thicker sandstone beds and uppermost coarse-grained cross-stratified sandstones. Towards the southwest of Domehar village, profuse development of soft-sedimentary deformation structures viz. load structures, dish and pillar structures, convolute lamination has been observed. The rocks are mainly medium- coarse-grained arkosic wackes. In the clayey matrix, grains have concavo-convex contact as well as sutured contact. The sedimentary rocks are poorly sorted, closely packed and have a greater proportion of clay (Sub arkosic and arkosic wacke). Most of the rocks in FA1a are not well sorted. The FA2a association comprises ripple-laminated sandstones (F3), tabular thick-bedded sandstones (F4) and cross-stratified sandstones (F5).

Ripple laminated sandstones (F3)

Description

This facies (F3) comprises coarsening-upward successions of light grey to greenish-grey coloured sandstones (thickness varies from 20 to 30cm), truncated by distributary channels (F1). Sandstones are well-sorted, medium- to coarse-grained, and intercalated with siltstone laminations (3–4cm thick) (Fig. 5a). The sandstone beds are about 30–60cm in thickness and extend laterally up to 3–4km. Very good exposures of F3 are found along Domehar–Chhaosha and Kuftu–Rauri road sections. This facies exhibits dominant asymmetrical ripple marks associated with current ripple cross-laminations (Fig. 5b). The amplitude of asymmetrical ripples ranges between 0.5 and 1.2 cm, wavelengths vary from 7 to 15cm and the thickness of current ripple cross-lamination varies from 1.5 to 2cm. Asymmetric ripples are bidirectional at some places (Fig. 5c). In some places, hummocky-cross-stratifications (HCS) are present within sand beds. Most of the sandstone beds have ball-and-pillow structures that load into the underlying silty intervals (Fig. 5d). Pillow structure is 15 to 20cm thick and laterally continuous for 25–30cm. Ball structures are generally 5–10cm thick and laterally continuous for 15–20cm.

Interpretation

The coarse and thick light grey to greenish coloured sandstone beds truncated by distributary channels (F1) have been identified as delta front deposits based on their vertical alignments and truncations (Uroza and Steel 2008; Chen et al. 2015; Peng et al. 2020). Dominance of asymmetrical ripples and current ripple cross-lamination indicates sand

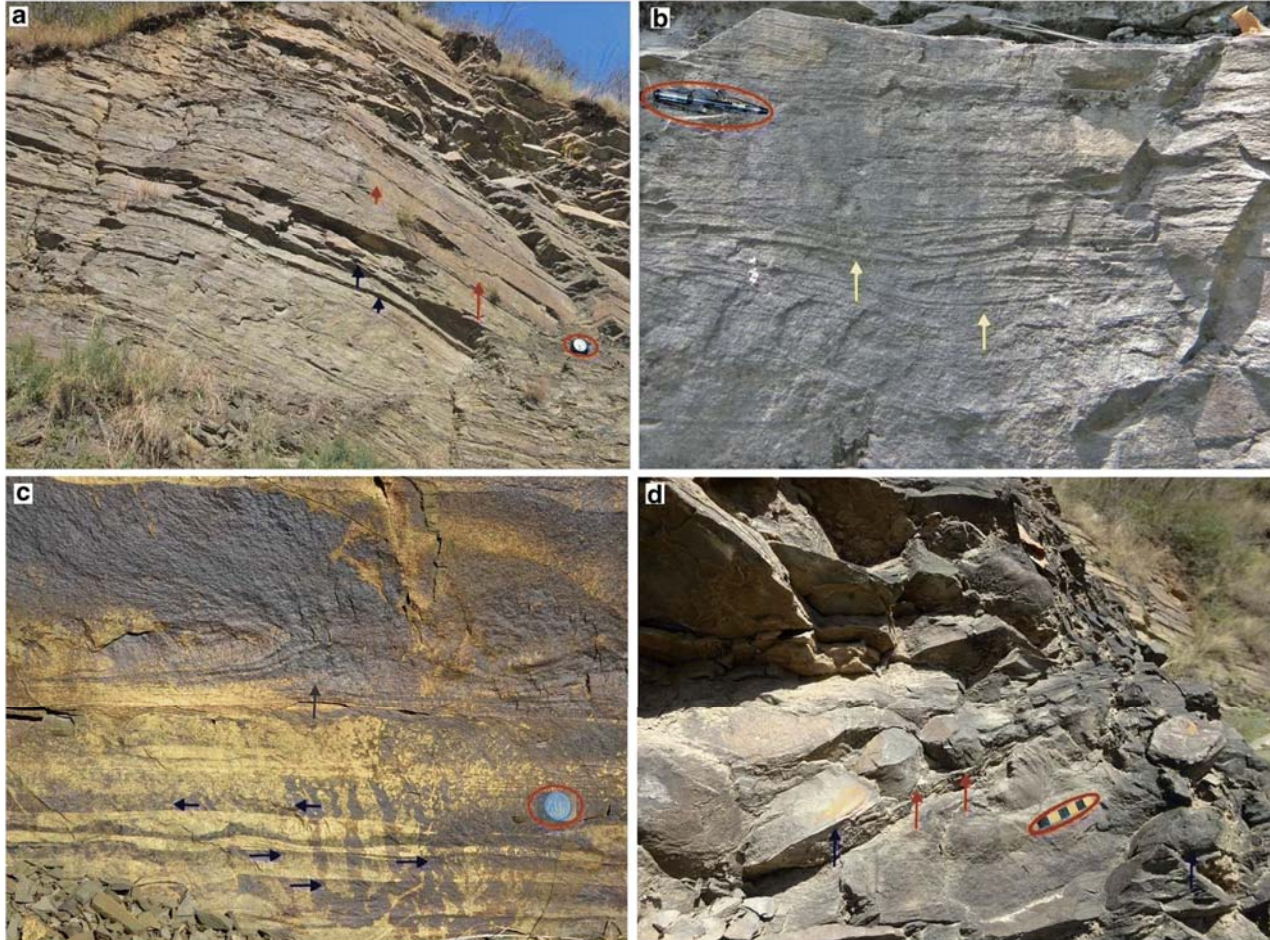


Fig. 5. Ripple laminated sandstones (F3) of proximal delta front deposit (FA2a) have been documented along Domehar–Chhaosa and Kufu–Rauri road sections. (a) Coarsening-upward, medium- to fine-grained ripple laminated sandstone units. Red arrows show sandstone units, and blue arrows mark siltstone units. Scale: length of the clinometer = 9cm. (b) Current ripple cross-laminations typical of facies F3. Yellow arrows mark the ripple cross-laminations. Scale: length of pen =15cm. (c) Preservation of bidirectional asymmetrical ripples and ripple cross-lamination within sandstone units. Blue arrows mark the direction of ripple migration. Scale: diameter of coin =3cm. (d) Profuse development of ball-and-pillow structures that load into the underlying silty intervals. Red arrows mark the ball structures and blue arrows mark the pillow structures. Scale: length of scale =5cm

deposition during ripple migration as a result of unidirectional subaqueous flow (Miall 1996; Magalhães et al. 2015; Van Cappelle et al. 2016). The presence of few bidirectional asymmetric ripples points towards the influence of tidal activity in F3 (Wilson 2005; Peng et al. 2018). The rare occurrences of HCS indicate the influence of hyperpycnal flows (Tinterri 2011; Basilici et al. 2012). The ball-and-pillow structures indicate slumping resulted due to gravity loading representing rapid sedimentation of unconsolidated sediments (Li et al. 2011; Plink-Bijörklund 2020; Peng et al. 2020).

Tabular thick-bedded sandstones (F4)

Description

This facies (F4) constitutes coarsening upward successions of grey to greenish-grey coloured sandstone beds having horizontal (with thin flakes of mud and mica) or low angle stratifications and displaying tabular extensive sheet-like geometry (Fig. 6a). The beds are 40–60 cm thick and laterally persistent for over 3–5 km. Sandstones of F4 are mainly trough cross-stratified (5–10cm thick and laterally continuous for 18–20cm) with erosional surfaces (Fig. 6b). Water escape structures (0.5–1cm thick), and load casts (10–15cm thick and laterally continuous for 20–25cm) are also common (Fig. 6c). F4 shows a prominent upward coarsening (along Ghanahatti–Gohri road transects), from wavy laminated muddy sediments to succeeding fine-grained sandstones with small cross-strata sets (0.2–0.3cm thick), and then to medium-grained sandstones with sigmoidal cross-stratifications which are 0.2–0.4cm thick, with uppermost coarse sandstones. Individual sandstone beds exhibit stratification with a thickness of 0.4–0.5cm, separated by mud drapes. Planar, parallel and wavy laminations are the main characteristics of the sand bodies. The scale of the sedimentary structures increases from ripple laminations, flasers and planar, parallel and low angle cross-laminations up to comparatively larger-scale cross-bed sets of 2.5–4 cm thickness. Bidirectional cross-stratifications (0.3–0.4cm thick) are also present at some places (Fig. 6d).

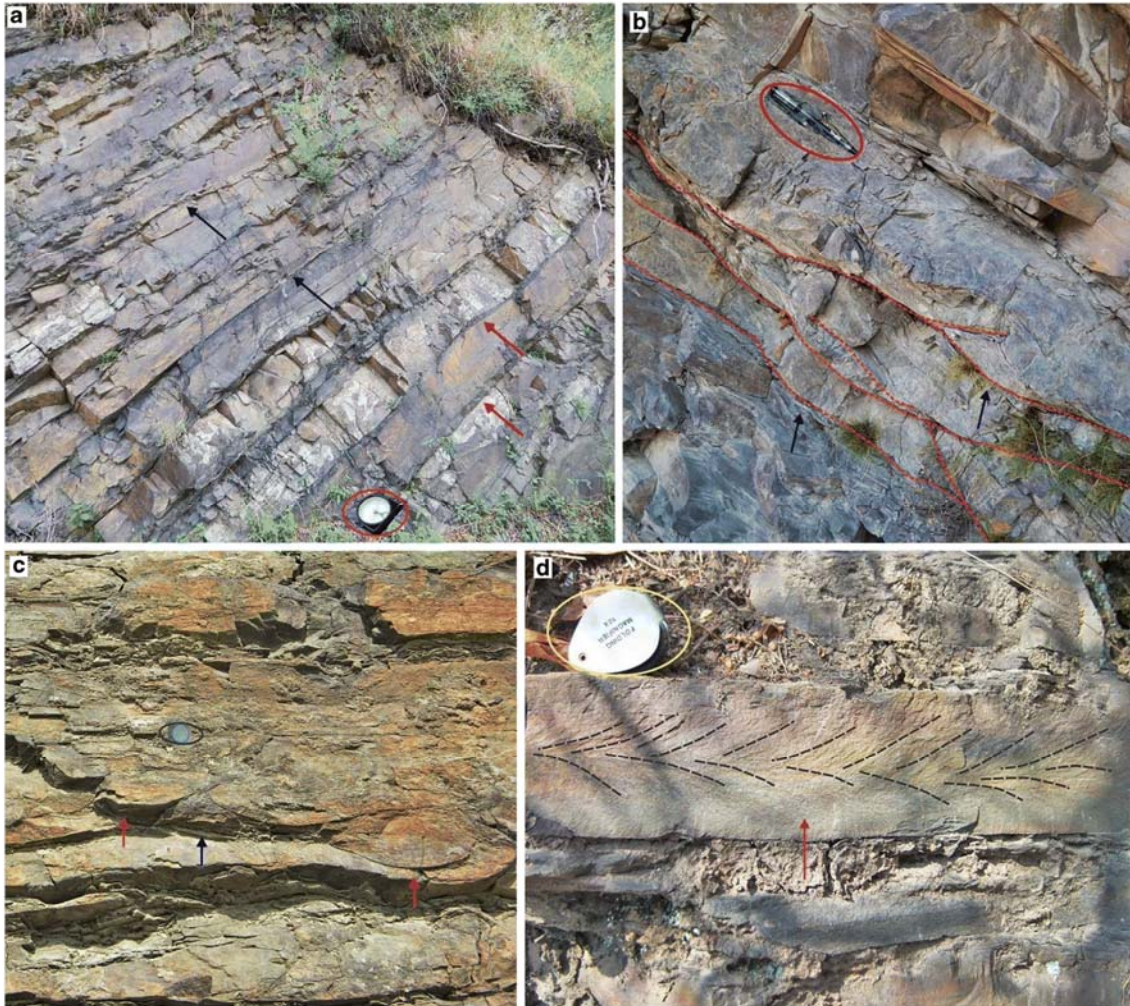


Fig. 6. Field photographs of tabular thick-bedded sandstones (F4) in proximal delta front deposit (FA2a) have been documented along Ghanahatti–Gohri road transects. (a) Tabular thick-bedded sandstones with thin laminated siltstones. Blue arrows indicate sandstone units, and pink arrows indicate thin siltstone units. Scale: length of clinometer = 9cm. (b) Trough cross-stratifications in sandstone units. Blue arrows mark the base of the troughs. Scale: length of pen =15cm. (c) Load structures and water escape structures. Red arrows indicate load structures and blue arrow shows water escape structure. Scale: diameter of coin =3cm. (d) Bidirectional cross-sets. Red arrow shows bidirectional cross-stratification. Scale: length of pocket lens =4cm

Interpretation

This facies (F4) reflects sediments deposited in terminal distributary channels (Olariu and Bhattacharya 2006; Buatois et al. 2012; Van Yperen et al. 2019). Laterally extensive, sheets of coarse-grained sandstones are deposited by unconfined flows (Eide et al. 2016). The erosional bases with abundant trough cross-strata, suggest terminal distributary channels (Olariu and Bhattacharya 2006; Ahmed et al. 2014; Johnson et al. 2016). Soft sedimentary deformation structures and plane-parallel laminations are deposited in a fluvially influenced depositional setups (Olariu and Bhattacharya 2006; Rana et al. 2016; Zhang et al. 2018). Development of rippled laminae, sigmoidal cross-bedding, flaser beds, bidirectional cross-strata, plane parallel lamination, the presence of mud drapes between stratification sets and low-angle lamination points towards a tidal origin in a shallow marine setup (Rossi and Steel 2016; Anell et al. 2020).

Cross-stratified sandstones (F5)

Description

Facies F5 comprises coarsening-upward successions of medium- to coarse-grained cross-bedded sandstones (15–20cm thick), traced along the Kanda–Kannair road section. Sandstones at basal intervals exhibit concave-up erosional surfaces. F5 is mainly characterized by sigmoidal cross-stratification (0.3–0.4cm thick), bidirectional cross-strata (0.2–0.3cm thick), plane-parallel laminated (0.2–0.4cm thick) sandstones. At places, sigmoidal cross-beddings with mud drapes have been recognized (Fig. 7a). Sandstones at upper intervals exhibit planar to undulatory parallel laminated beds deposited over scoured surfaces resembling swales (SCS) (10–12cm thick and laterally continuous for 25–30cm). Convex upward laminae with flat bases and internal stratifications (hummocks) (10–15cm thick and laterally continuous for 20–25cm) are moderately abundant in outcrop sections (Fig. 7b). The swales in cross-stratified sandstones of F5 transition upward into hummocky cross-stratified sandstones. Planar-laminated sandstone intervals are approximately 2–4m thick in outcrop sections (Fig. 7c). Occasionally, hummocky cross-stratified sandstones are associated with asymmetric ripples filled up with muddy units. Cross-set thicknesses vary between 5 and 10cm. Syneresis cracks (0.5–1cm thick) are locally present (Fig. 7d). Soft sedimentary deformational structures like load structures (15–18cm thick and laterally continuous for 25–30cm), water-escape structures (1–2cm thick) and dish and pillar structures (10–12cm thick and laterally continuous for 20–25cm) are recorded at few intervals.

Interpretation

The coarsening-upward depositional trend of cross-stratified sandstones of F5 attests to deposition in tide-dominated delta front, intensely reworked by mouthbars (Anell et al. 2020). Concave-up erosional surfaces are indicative of terminal distributary channels (Ahmed et al. 2014; Johnson et al. 2016). The close association of mouthbars and distributary channels point towards a proximal delta front depositional environment (Ahmed et al. 2014). The abundance of sigmoidal cross-stratification, bidirectional cross-strata and mud drapes indicate deposition of F5 in shallow-marine setups with tidal influence (Allen and Honewood 1984; Plint and Wadsworth 2003; Rossi and Steel 2016; Anell et al. 2020). The stacked sandstones with HCS, SCS represents deposition by high-energy oscillatory currents, in storm-influenced middle-lower shoreface settings at intervals of fair-weather wave base and storm wave base (Li et al. 2011; Bowman and Johnson 2014). Sandstones with parallel laminations reflect deposition in the upper-flow-regime (Tunbridge 1981; Plink-Björklund 2005; Kiwango and Mishra 2020). The cross-stratification with symmetric ripples indicates a wave-dominated process (Gani and Bhattacharya 2007; Peng et al. 2018). Syneresis cracks reflect short phases of salinity reduction (Plummer and Gostin 1981; Buatois et al. 2012). A high rate of sedimentation along an unstable slope led to the deposition of soft-sediment deformation structures (Carmona et al. 2009; Buatois et al. 2012).

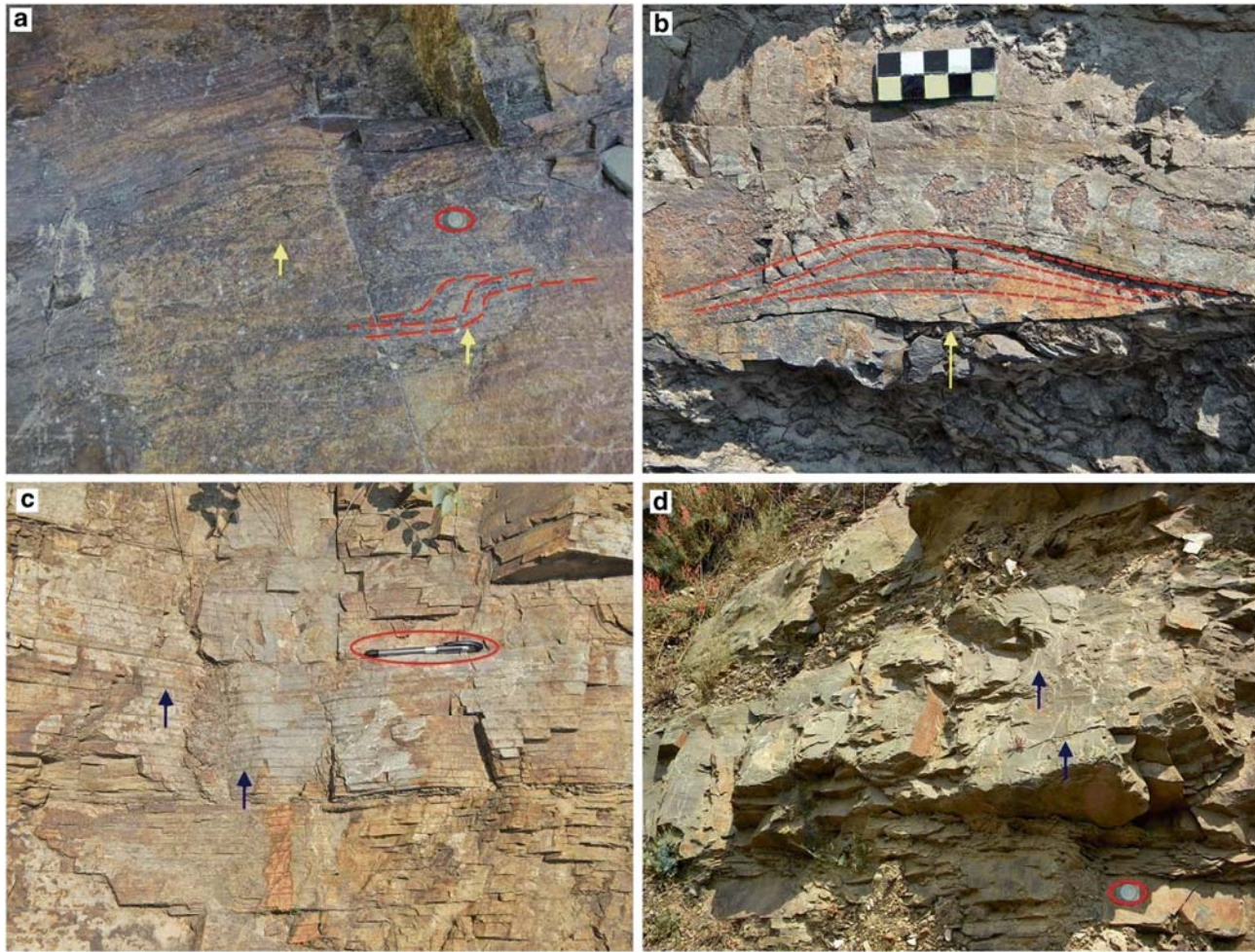


Fig. 7. Cross-stratified sandstones (F5) of proximal delta front deposit (FA2a), traced along Kandaghat–Kannair road section. (a) Abundance of sigmoidal cross-stratification indicates the influence of tidal activity. Yellow arrows show sigmoidal cross-stratifications. Scale: diameter of coin =3cm. (b) Hummocky cross-stratifications. Yellow arrow marks the flat base of hummock. Scale: length of scale =5cm. (c) Planar-laminated sandstones. Blue arrows show planar laminations. Scale: length of the pen =15cm. (d) Syneresis cracks are locally present. Blue arrows show syneresis cracks. Scale: diameter of coin =3cm

Distal delta front (FA2b)

FA2b comprises 3–4-m thick cross-stratified sand bodies in the upper part and fine siltstones in the lower part of the succession. FA2b extends laterally up to hundreds of metres along Khiari–Miaon and Dangi–Tudul road sections and in and around Kohbag and Jodhana village. The fine-grained siltstones in the lower part are closely packed and mainly consist of quartz. Three major facies attributes have been delineated from the study area: wavy-bedded sandstone and mudstone (F6), heterolithic sandstone-prone thin units (F7) and sheet-like heterolithic units (F8).

Wavy-bedded sandstone and mudstone (F6)

Description

This facies (F6) consists of a coarsening upward sand dominated succession characterized by moderately sorted to well-sorted buff to khaki green coloured interbeds of sandstones (5–30cm thick) and mudstones (1–10 cm thick). Interbedded fine-grained sandstone–mudstone exhibit wavy geometry (Fig. 8a), well documented along Khiari–Miaon transects.

Symmetrical ripples (Fig. 8b) with amplitude ranges between 0.5 and 1 cm and wavelength ranges from 3 to 4 cm are observed within some sandstone units. The basal sand bodies show intense soft-sediment deformation structures (load casts, pseudonodules). The upper units preserve mud flasers along the foresets and asymmetrical current ripples (Fig. 8c). In some places, rare occurrences of low angle cross-stratified (Fig. 8d) and hummocky cross-stratified beddings are also observed.

Interpretation

F6 attest to sedimentation in a wave-influenced middle delta front (Lee et al. 2005). Intermittent mudstone layers within sandstones demonstrate oscillating energy conditions (Todd 1996; Magalhães et al. 2015). The presence of symmetrical ripples within some sandstone units indicates F6 is locally influenced by wave action (Carmona et al. 2009; Anell et al. 2020). Rapid sedimentation resulted in profuse development of different types of load structures (Buatois et al. 2012). The existence of mud drapes over cross-laminations and asymmetrical current ripples suggests deposition by fluctuating mechanisms of subaqueous traction and suspension (Miall 1996; Magalhães et al. 2015; Eltayib et al. 2018). Low angle cross-stratified and hummocky cross-stratified beddings are deposited by storm waves (Dumas et al. 2005; Legler et al. 2014).

Heterolithic sandstone-prone thin units (F7)

Description

F7 comprises coarsening- upward successions (2–16 m thick) of sandstone-dominated intervals which are laterally exposed approximately 6–7 km along the Dangi–Tudul road section. Intervening mudstones are generally grey in colour and range in thickness from 4 to 22 cm. The sandstone intervals are generally enclosed by mudstone layers (Fig. 9a). The sandstone units preserve continuous alternation of parallel laminations (0.3–0.4cm thick) (Fig. 9b) and climbing ripple laminations (0.5–0.8cm thick) (Fig. 9c). Syneresis cracks (1–4cm

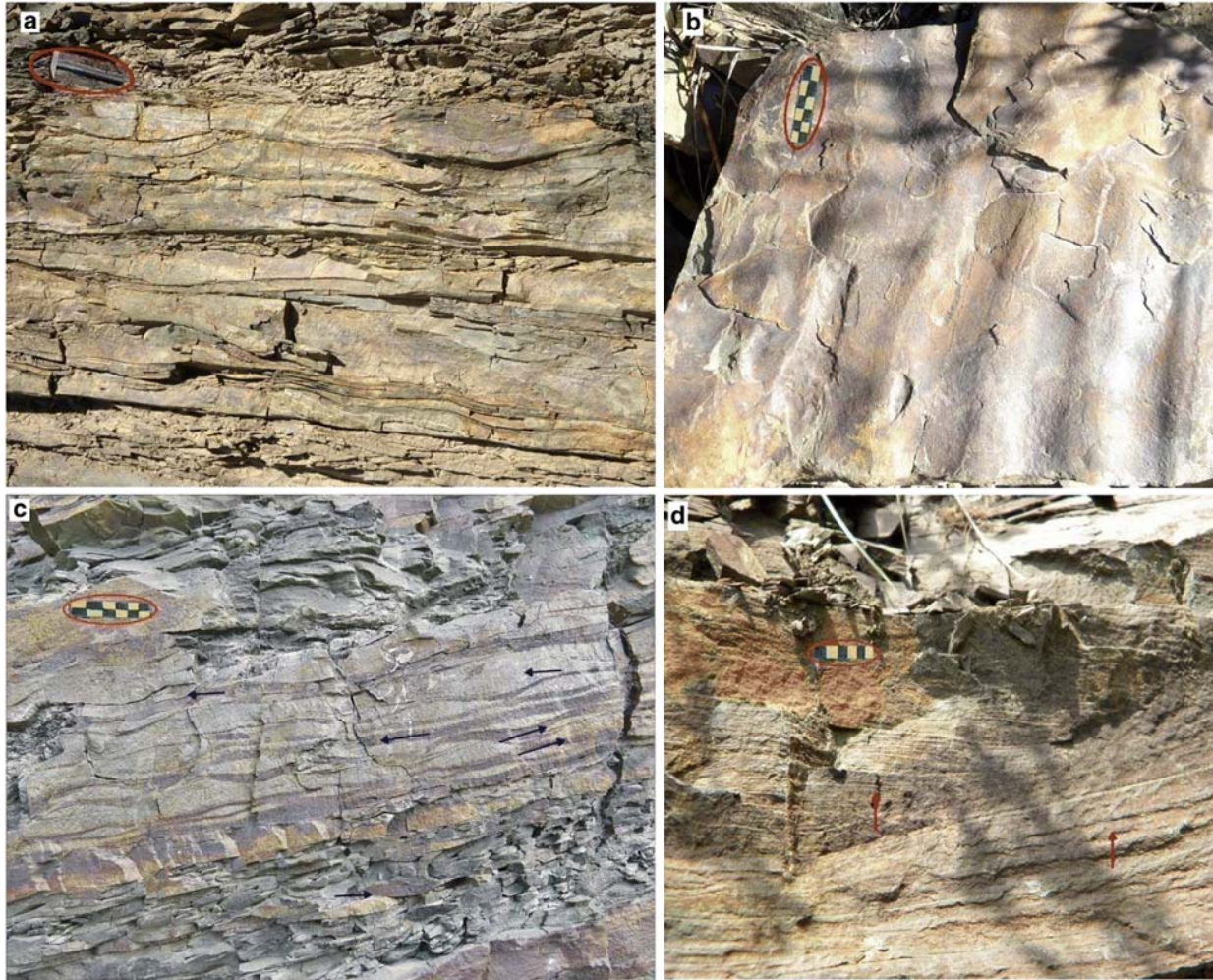


Fig. 8. Wavy-bedded sandstone and mudstone facies (F6) of distal delta front deposit (FA2b), documented along Khiari–Miaon transects. **(a)** Interbedded fine-grained sandstone–mudstone exhibit wavy geometry. Scale: length of hammer =32.5cm. **(b)** Symmetrical ripples within sandstone units. Scale: length of scale =7cm. **(c)** Asymmetrical current ripples. Scale: 7cm, blue arrows indicate direction of ripple migration. **(d)** Rare occurrences of low angle cross-stratifications. Red arrow shows low angle cross-stratifications. Scale: length of scale =6cm



Fig. 9. Heterolithic sandstone-prone thin units (F7) of distal delta front deposit (FA2b), exposed along Dangi–Tudul road section. **(a)** Sandstone-dominated heterolithic units. Red arrow indicates sandy units and yellow arrows show silty-muddy units. Scale: height of the person =1.3m. **(b)** Sandstones exhibit parallel laminations. Blue arrows indicate parallel laminations. Scale: length of pen =15cm. **(c)** Climbing ripple laminations. Scale: length of scale =6cm. **(d)** Sole marks are locally present at the base of sandstone intervals. Blue arrows mark the sole marks. Scale: length of scale =6cm

thick) are locally present within sandstone–mudstone intervals. Sharp-based sand beds (10–12cm thick) comprise symmetrical ripple lamination (0.2–0.3cm thick). Some mud intervals exhibit occurrences of fine sand lenses (0.8 to 1.5 cm thick and laterally extends 1–2cm). The flute casts are 2–3cm thick and groove marks are 1–2cm thick (Fig. 9d). Soft-sedimentary deformation structures (mainly loading) are present throughout the facies. The sandstone beds are sharply scoured based and contain sole marks (flutes and groove marks).

Interpretation

The upward-coarsening depositional trend generally indicates a progradational depositional system (Olariu et al. 2010; Ainsworth et al. 2016). The interbedding characteristics reflect periodic deposition in a distal delta front below the fair-weather wave base (Ahmed et al. 2014). Continual preservation of alternated parallel lamination and climbing ripple lamination indicates towards flows with variable velocities (Mutti et al. 2003; Bowman and Johnson 2014). Short-lived intervals of salinity reduction are represented by the rare presence of syneresis cracks (Vakarelov et al. 2012; Mode et al. 2018). Prominent scoured bases, dominance of low angle stratified units (at places hummocky cross stratified) indicates occasional storm-wave activity (Clifton 2006; Buatois et al. 2012). Symmetrical wave ripples are the possible indicators of local wave influence (Anell et al. 2020). Preservation of fine sand lenses within muddy intervals indicates that they have been developed by distal density currents (Smyrak-Sikora et al. 2019). The flute casts, sole marks and underlying mudstone layers suggest an initial turbulent stage which was later possibly followed by a depositional stage of low concentration turbidity currents (Puigdomenech et al. 2014). The erosional thick sandstone beds containing soft-sediment deformation structures in F7 are probably indicative of rapid deposition by dense hyperpycnal gravity flow in a steep slope (Mulder et al. 2003; Mutti et al. 2003; Smyrak-Sikora et al. 2019).

Sheet-like heterolithic units (F8)

Description

This facies (F8) consists of successive thinly interbedded 2 to 6 m thick, laterally extensive (6–7km) sandstones–siltstones and mudstones (Fig. 10a), near Jodhana village. Mudstones account for about 40–50% of the lithofacies and the rest is composed of sandstones and siltstones. At places, sandstone units exhibit profuse development of soft sedimentary deformation structure (slump folds) (Fig. 10b). Slump folds are 1.5–3cm thick and laterally continuous for 12–15cm. The sandstone–siltstone and mudstone layers often form couplets that are 4–5 m thick with flaser bedding (0.5–1.5cm thick) (Fig. 10c). From the basal part of the interbedded units to the top, the sandy intervals are planar laminated to the current ripple cross-laminated. However, sandstones exhibiting cross stratifications (0.3–0.4cm thick) with mud flasers (Fig. 10d) are common at the base of laterally extensive heteroliths.

Interpretation

Sheet-like geometry and interbedded heteroliths suggest F8 deposited in a distal delta front depositional environment below the wave base (Chen et al. 2015). Abundance of mud units

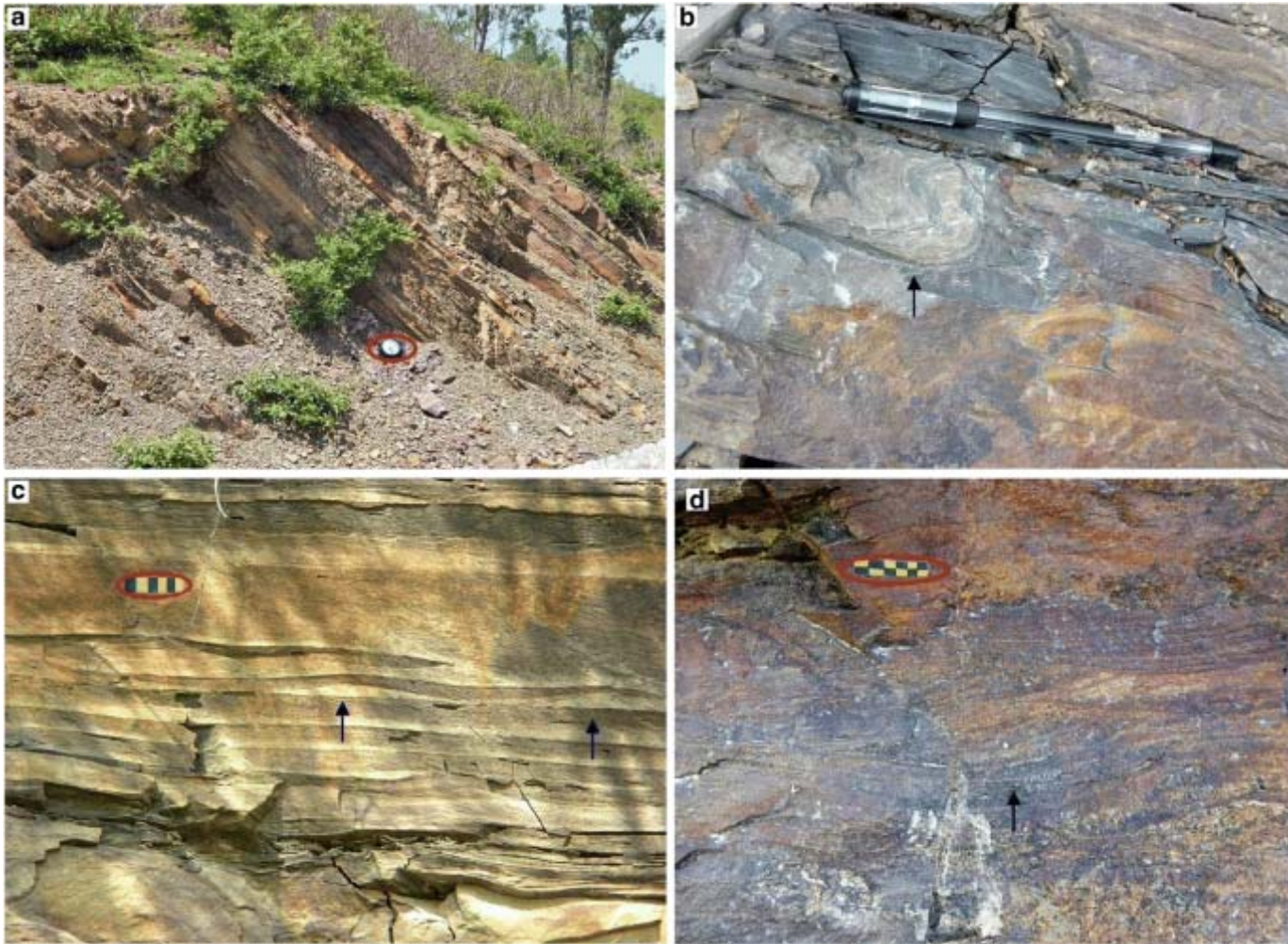


Fig. 10. Field photographs of sheet-like heterolithic units (F8) of distal delta front deposit (FA2b) have been observed near Jodhana village. **(a)** Thinly interbedded sandstones–siltstones and mudstone units displaying sheet-like geometry. Scale: length of clinometer =10cm. **(b)** Sandstone units exhibit the development of slump folds. Blue arrow indicates slump folds. Scale: length of pen =15cm. **(c)** Flaser beddings. Blue arrows mark flaser bedding. Scale: length of scale =4cm. **(d)** Cross-stratifications with mud flasers are common at the base of heteroliths. Blue arrow shows mud flasers. Scale: length of scale =7cm

and soft sedimentary deformation structures, slump folds signifies low-energy slope sedimentation (thickness of the slope varies randomly) (Bowman and Johnson 2014; Kundu et al. 2011; Rana et al. 2016). Occurrence of flaser bedding also points to tidal activities (Allen 1980; Visser 1980; Van Yperen et al. 2020). Sandy intervals with planer laminations and current ripple cross-laminations are indicating that the velocities of the flows changes periodically (Mutti et al. 2003; Bowman and Johnson 2014). Cross-stratified sandstones with mud flasers attest to suspension settling at a standstill condition of water probably due to change in directions of tidal currents (Olariu et al. 2012).

Prodelta deposits (FA3)

This facies association consists of mud–sand couplet facies (F9), interbedded mudstone–siltstone and fine-grained sandstone facies (F10), and rhythmically laminated sandstone and mudstone (F11). FA3 deposits are observed in and around Ukhru, Chayabag, Kothighati village and along the Chhaosa–Baliana, Bog–Arki, Rouri–Arki transects (Fig. 2). The distal part of the prodeltaic succession in the study area is mainly represented by FA3 deposits. FA3 is represented by quartz wackes and quartz arenites. The rocks are generally fine-grained and moderately sorted. The matrix in the arenites is sericitic and in some places quartzo feldspathic. Rock fragments of mudrocks occur occasionally.

Sand–mud couplets (F9)

Description

The sandy-muddy intervals of (F9) are well recorded in and around Ukhru village (Fig. 11a). The sandstones are fine-grained (10 to 18 cm thick) and generally enclosed by mud layers. Mud layers (generally grey in colour) range from 2 to 5cm in thickness. Interlaminated sandstones and siltstones with rounded crested asymmetrical ripples (combined-flow ripples) are common occurrences in the sandstone units (Fig. 11b). The amplitude and wavelength of the ripples approximately vary from 2 to 2.5cm and 8–10cm respectively. The dimensions of the mud flasers vary from 0.3 to 0.9cm. The sand–mud couplets exhibit occurrences of scours, normal and inverse grading, planar to low-angle cross-laminations. The sandstone and mudstone layers in the heteroliths form flaser, lenticular and wavy bedding (Figs. 11c). Load structures and convolute laminations occur as soft sedimentary deformation structures in many intervals (Fig. 11d).

Interpretation

The laminated sand–mud couplets reflect periodic flow activity associated with repetitive slack water sedimentation which led to the suspension of finer sediments (Reineck and Singh 1980; Waresak 2016). The presence of combined-flow ripples within F9 represents variations in flow velocity during their deposition (Dumas et al. 2005; Basilici et al. 2012). Variations in the geometry of the beds and laminations containing scours, normal and inverse grading, planar to low-angle cross-laminations are indicative of turbulent flow deposits reflecting a continuous effect of waxing and waning of currents (Wilson and Schieber 2014). The flaser, wavy and lenticular bedding indicates a tidal deposition setting (Reineck and Wunderlich 1968; Rahman et al. 2009; Khanam et al. 2017). Load structures

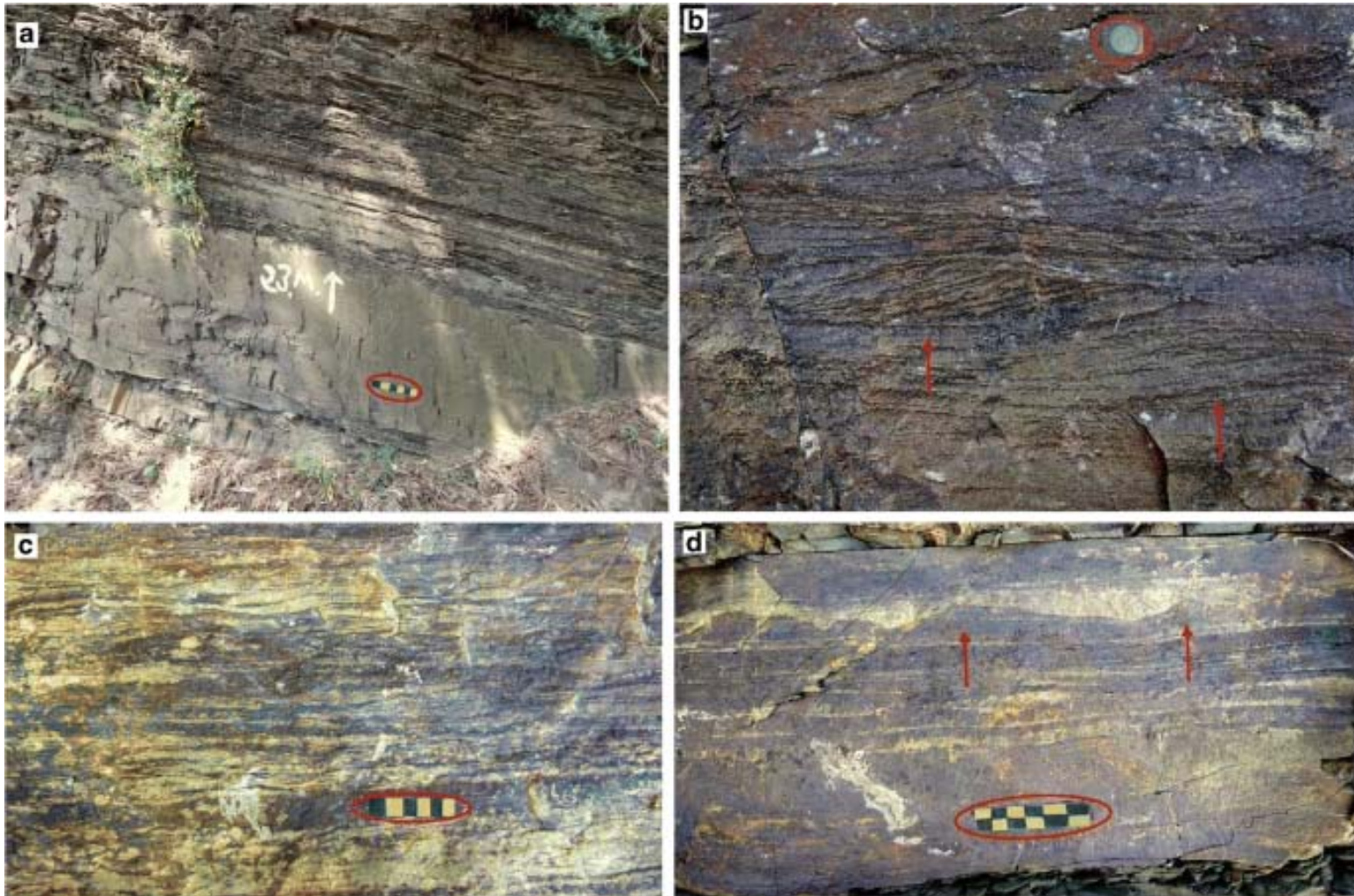


Fig. 11. Sand–mud couplets (F9) in prodelta deposits (FA3) have been documented in and around Ukhru village. (a) Sand–mud couplets. Scale: length of scale =6cm. (b) Combined-flow ripples are common occurrences in F9. Red arrows show combined-flow ripples. Scale: diameter of coin =3cm. (c) The sandstone and mudstone layers in the heteroliths form flaser beddings. Scale: length of scale: 6cm. (d) Convolute laminations. Red arrows indicate convolute laminations. Scale: length of scale 7cm

and convolute laminations occurring as soft sedimentary deformation structures are likely to be a product of deltaic depositional setup where the rate of sedimentation is higher (Buatois et al. 2012).

Interbedded siltstone and fine-grained sandstones (F10)

Description

This facies (F10) mainly comprises 3–6 m thick successions of interbedded siltstones and fine-grained rippled sandstones. Good exposures of F10 have been observed in and around Chayabag village along the Bog–Arki road section (Fig. 12a). The upper intervals are characterized by 2–3m thickening and coarsening upward mud dominated siltstones which grades into hummocky cross-stratified sandstones (Fig. 12b) which possess sharp bases represented by sole marks. In few intervals of successions of F10, the sandstones are observed as inversely graded (0.6–0.9cm thick) exhibiting increase in grain size from the base of the unit towards the top of the unit (Fig. 12c). Starved current ripples (Fig. 12d) with amplitude 0.5cm to 2cm and wavelength 3cm to 4cm are also present.

Interpretation

The rhythmites of sandstone–siltstone are indicative of fluctuations in energy condition; the thinner intervals of sand–silt are a product of suspension settling of sediment due to gravity loading whereas the comparatively thick rippled sandstone beds are deposited by fluvial flood (Bhattacharya (Eide et al. 2016)). The presence of HCS in a few sandy intervals indicates a wave-storm influenced depositional setting (Walker and Plint 1992; Johnson and Baldwin 1996; Eriksson et al. 1998; Leren et al. 2010; Li et al. 2015). Abundance of inverse grading at the bases of the heterolithic intervals is probably indicative of acceleration of the flow velocities (Kneller 1995; Basilici et al. 2012; Saitoh and Masuda 2013). The presence of starved wave ripples reflects periodic storm (Ahmed et al. 2014). F10 exhibiting overall coarsening upward trend indicates deposition along the distal zone of a prograding delta.

Rhythmically laminated sandstone and mudstone (F11)

Description

F11 is characterized by fine- to very fine- sandstone and mudstone units which are thinly laminated (Fig. 13a). Heterolithic units range in thickness from 1 to 10cm. This facies occurs mainly in and around Kothighati village. F11 is volumetrically dominated by flaser, lenticular and wavy beddings. Lower intervals exhibit rhythmic occurrences of small scale (amplitude ranges 0.1–0.2cm from and wavelength 0.5–0.8cm) climbing ripple cross-laminations (Fig. 13b). Few sandstone beds exhibit symmetrical ripples. Mudstone beds generally preserved abundant sand loading which induced soft sedimentary deformation structures like convolute lamination, ball-and-pillow, and pseudonodules (Fig. 13c). Wrinkle marks and syneresis cracks are observed locally (near Kohbag village) (Fig. 13d).

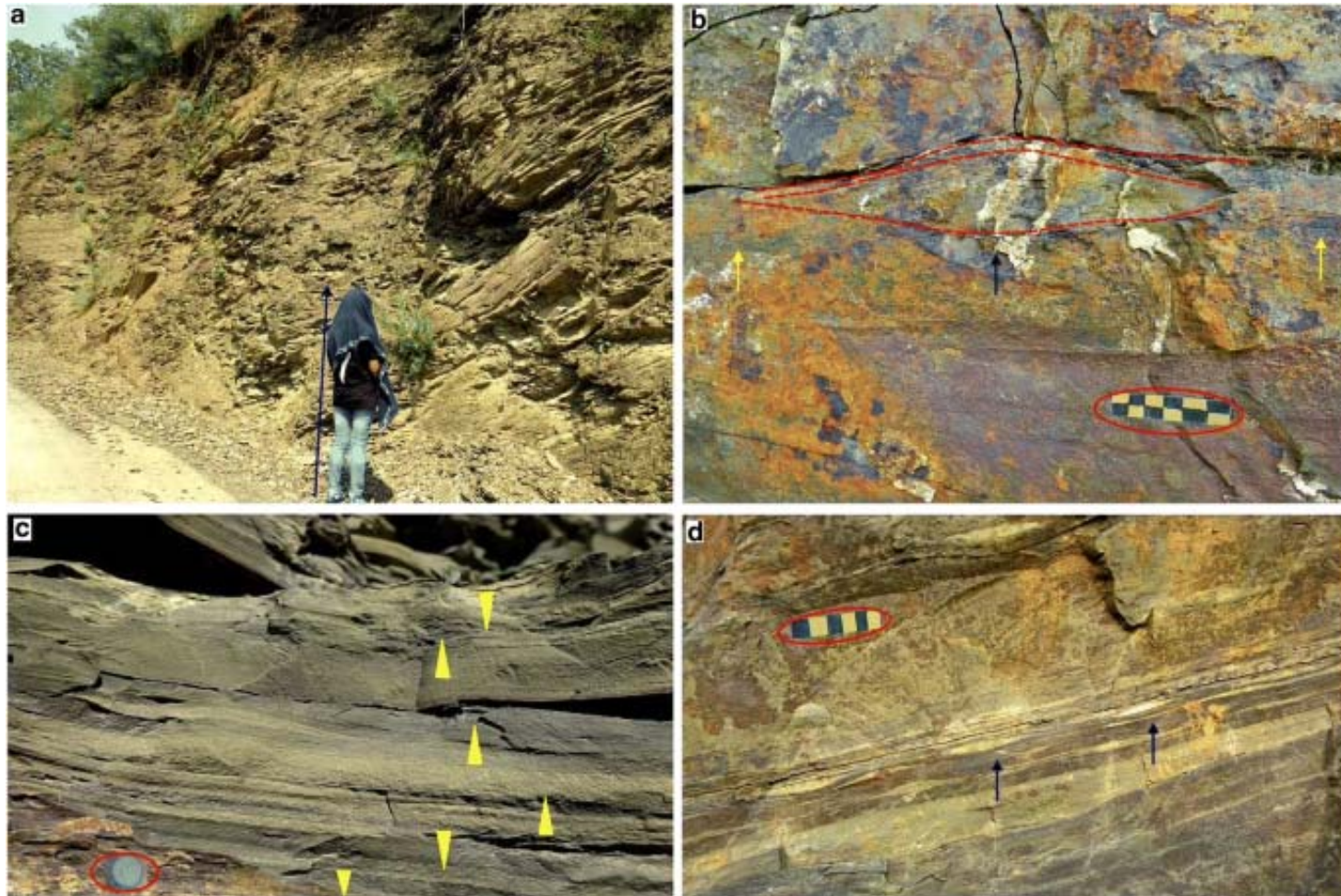


Fig. 12. Field photographs of interbedded siltstone and fine-grained sandstones (F10) of prodelta deposits (FA3), traced along the Bog–Arki road section. **(a)** Interbedded siltstones and fine-grained sandstones are indicative of fluctuations in energy conditions. Scale: height of the person 1.6m. **(b)** Hummocky cross-stratified fine-grained sandstones. Blue arrow indicates hummock and red arrows indicate swales. Scale: length of scale =7cm. **(c)** Sandstones are exhibiting inverse and normal grading. Yellow arrows indicate inverse and normal grading. Scale: diameter of coin =3cm. **(d)** The presence of starved wave ripples reflects periodic storm activity. Scale: length of scale =6cm

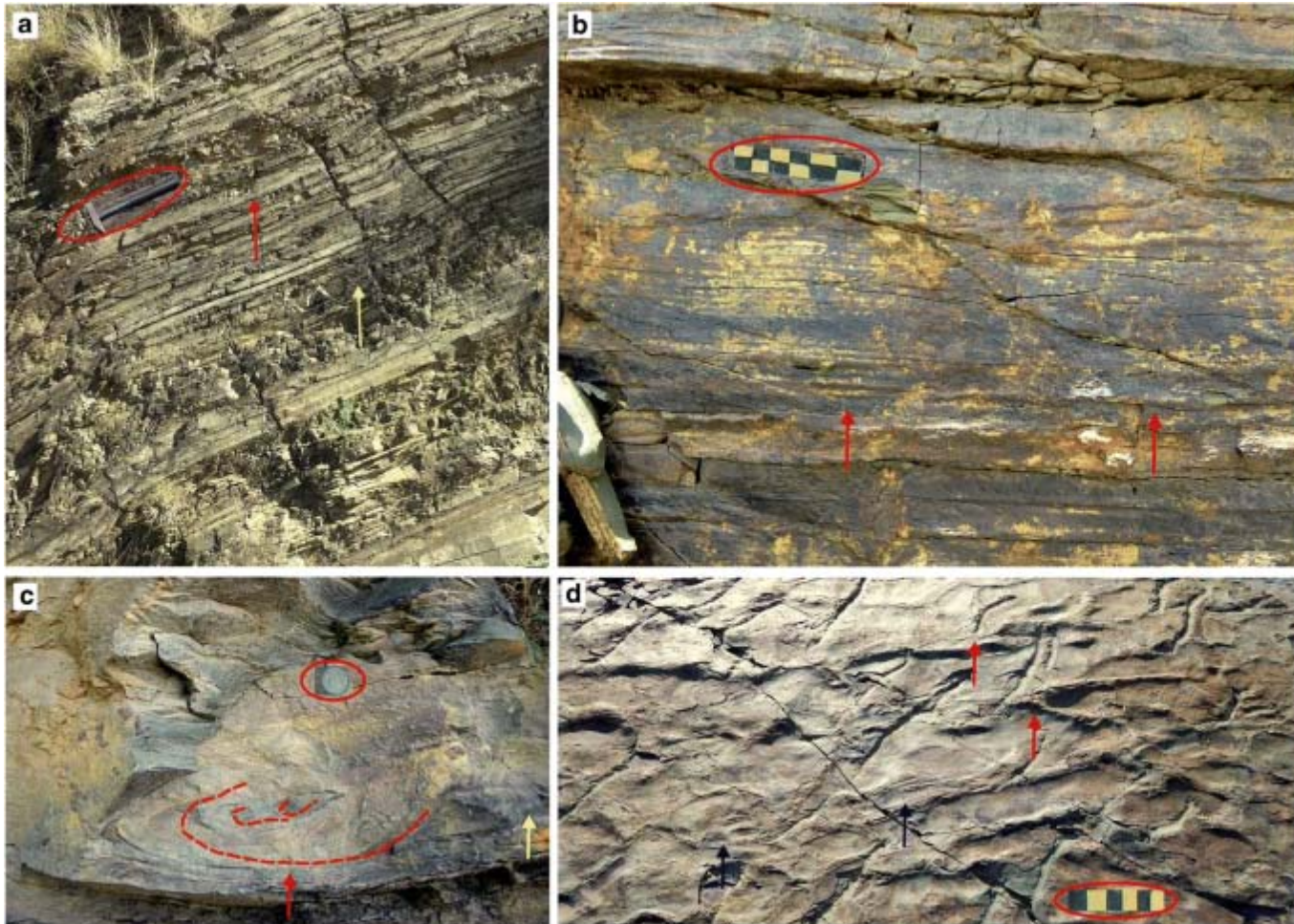


Fig. 13. Rhythmically laminated sandstone and mudstones (F11) of prodelta deposit (FA3) have been documented in and around Kothighati village. (a) Tidal rhythmites. Red arrow indicates sand units and yellow arrow shows mud units. Scale: length of hammer 32.5cm. (b) Rhythmic occurrences of climbing ripple cross-laminations. Red arrows show climbing ripple cross-laminations. Scale: length of scale 7cm. (c) Pseudonodule structures and slump folds. Red arrow indicates pseudonodule and yellow arrow mark the slump folds. Scale: diameter of coin =3cm. (d) Wrinkle marks and syneresis cracks. Red arrows indicate syneresis cracks and blue arrows show wrinkle structures. Scale: length of scale 6cm

Interpretation

The laterally extensive rhythmites of sand and mud exhibiting continuous variation in thickness reflect fluctuations in energy conditions caused by tidal currents (Kvale et al. 1989; Cummings et al. 2006; Gani and Bhattacharya 2007; Feldman et al. 2014). Profuse development of flaser, lenticular and wavy beddings within laminated sand–mud units indicate towards tidal origin (Williams 1991; O'Connell et al. 2017). Small scale rhythmic climbing ripple-laminations are indicative of strong tidal origin (Choi 2010; Choi 2011). Abundance of soft-sediment deformation structures reflects rapid sedimentation along relatively steep slopes (Buatois et al. 2012). The appearance of the wrinkle structures on the upper surface of the beds is probably generated by low energy wave currents or action of wave currents on cohesive mat layers (Sarkar et al. 2008, Sarkar et al. 2014; Samanta et al. 2016). Syneresis cracks reflect accelerated reversals in salinity conditions (MacEachern and Pemberton 1994; Buatois and Mángano 2003; Buatois et al. 2011; Taral and Chakraborty 2018) in intertidal zones. F11 is therefore interpreted as a tidal rhythmite (Williams 1989; Kvale 2003; Mángano and Buatois 2004; Mazumder and Arima 2005; Cummings et al. 2006; Eilertsen et al. 2011).

Process summary

Outcrop-based facies analysis reveals that the Chhaosa Formation represents a typical representation of a mixed-energy depositional setup which includes the interplay of different depositional processes in different scales. The outcrops of Chhaosa delta systems prominently display typical characteristics of a mixed-energy depositional system (Figs. 14 and 15) and thereby indicate that this ancient delta system is quite characteristically distinct from the ideal river-dominated, tide-dominated and wave-dominated deltas.

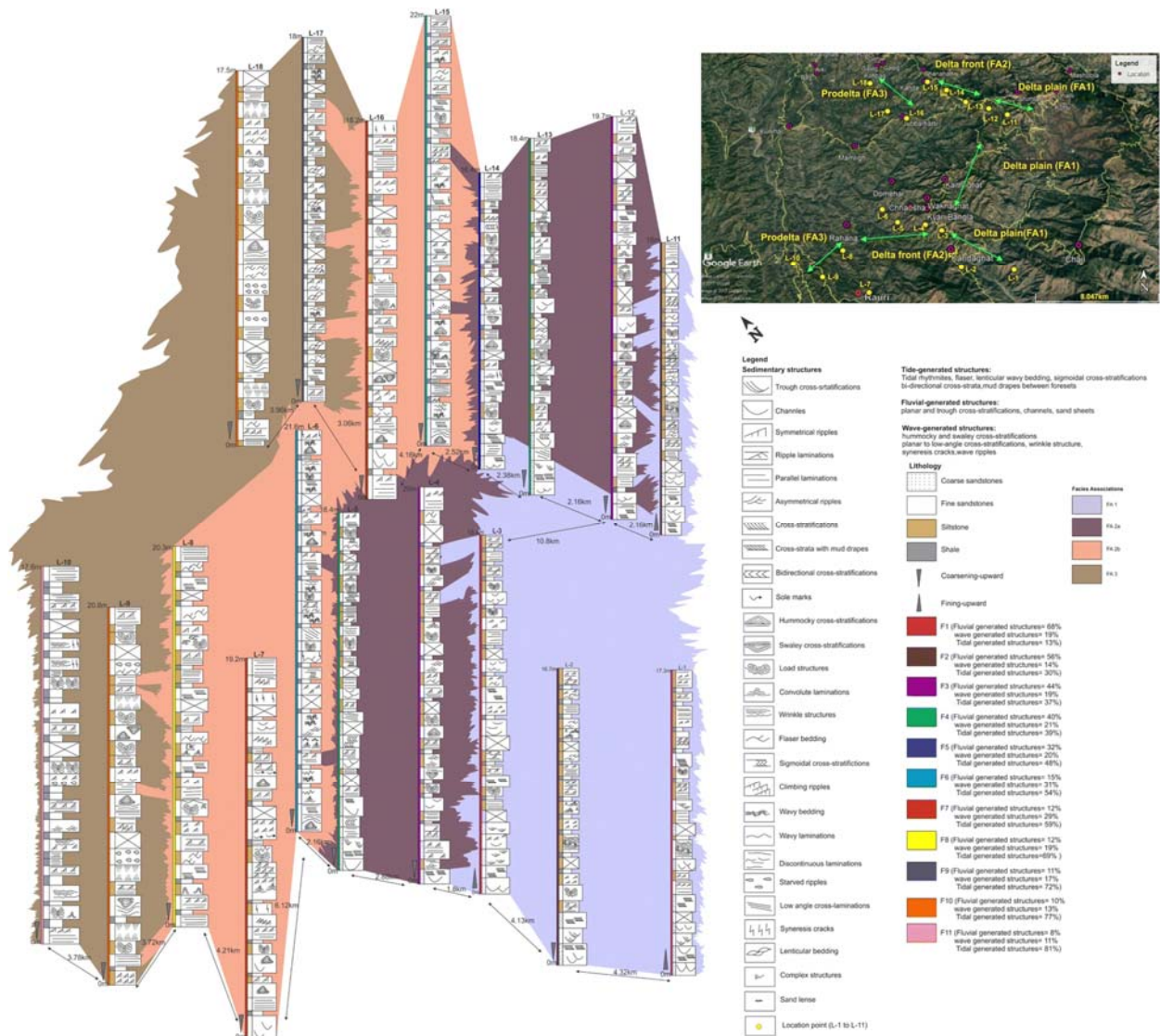


Fig. 14. Correlation panel based on measured sections (L-1 to L-18) represents the disposition of different lithofacies and lithofacies associations and their spatial and temporal relationship recorded in the Chhaosa delta system. Different colours have been used to indicate different lithofacies and lithofacies associations. The distribution of sedimentary structures across the outcrop sections of the study area reveals that they have been deposited by tidal (50.04%), fluvial (30.83%) and wave (19.13%) processes. Overall coarsening-upward succession represents progradational stacking pattern of a mixed-energy delta deposit (from prodelta (FA3) to delta front (FA2) to delta plain (FA1) deposit of the Chhaosa). The outcrop belt is approximately 63,520m long and the total stratigraphic thickness is about 1100m

Three major depositional processes have been determined: tidal (50.04%), fluvial (30.83%) and wave (19.13%) activity. The individual depositional processes exhibit a change in a typical pattern during marine-fluvial transitional period. A signature of wind action, though present, is deemed insignificant. The interaction of these processes has an important role indeed in the generation of the dominant facies associations identified (FA1, FA2 and FA3), characterising distinctive sub-environments, i.e. delta plain (FA1), proximal delta front (FA2a), distal delta front (FA2b) and prodelta (FA3). Coastal process classification ternary plots (modified after Galloway 1975, Ainsworth et al. 2011) have been constructed to understand the interplay of tide, fluvial and wave energy throughout the study area (Fig.

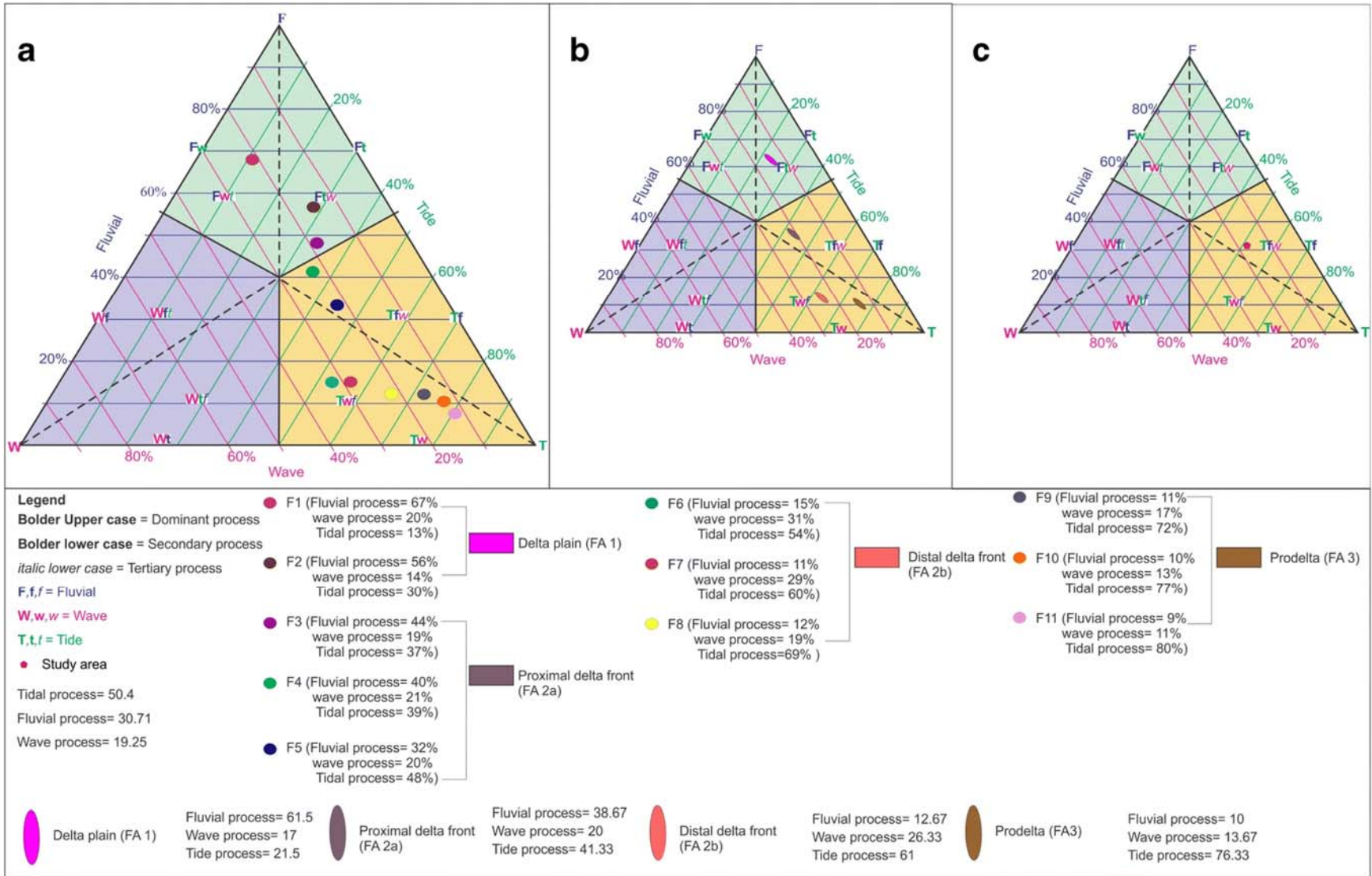


Fig. 15. Coastal process classification ternary plots (modified after Galloway 1975 and Ainsworth et al. 2011) of Chhaosa delta system, representing the interplay of tide, fluvial and wave energy throughout the study area. The basal part of the triangles indicates classification of non-fluvial shorelines. Apart from the basal line of the triangles, all the lines exhibit a few amount of fluvial activity. Similarly, lines on the left part of the triangles denote decreasing tidal activity, and lines on the right part represent decreasing wave activity. The ternary plots represent a simplified classification that emphasis the classification of predominant, secondary and minor processes and explains the way of counting percentages of sedimentary structures of different lithofacies and lithofacies associations from the study area (Fig. 14), which can be framed on the diagrams. F = dominance of fluvial activity; W = dominance of wave activity; T = Dominance of tide activity; Fw = Fluvial energy is predominantly present with influence of wave-activity; Ft= Fluvial energy is predominantly present with influence of tide activity; Tf = Tidal energy is predominant with influence of fluvial energy; Tw = Tidal energy is predominant with influence of wave activity; Wt = Wave energy is predominant with tidal influence; Wf = Wave energy is predominant with influence of fluvial activity; Fwt = Fluvial energy is predominantly present with wave influence and minor tidal activity; Ftw = Fluvial energy is predominantly present with tide influence and minor wave activity; Tfw = Tidal energy predominantly present with fluvial influence and minor wave activity; Twf = Tidal energy predominantly present with wave influence and minor fluvial activity; Wtf = Wave energy is predominantly present with tide influence and minor fluvial activity; Wft = Wave energy is predominantly present with fluvial influence and minor tide activity; fw = influence of fluvial and wave-activity; tf = influence of tide- and fluvial activity; wt = influence of wave and tide- activity; fwt = influence of fluvial, wave and tidal activity; Twf = Tide is the primary and wave and fluvial are secondary processes; Wtf = Wave is primarily present, and tide and fluvial are secondary processes. (a) The ternary plot represents the percentage of tide fluvial and wave energy processes in eleven lithofacies from the chosen outcrop sections of the study area and they have been marked by different colours. (b) The ternary plot represents percentages of tide fluvial and wave energy process in different facies associations, i.e. delta plain (FA1), proximal delta front (FA2a), distal delta front (FA2b) and prodelta (FA3) deposits and they have been marked by different colours. (c) The ternary plot represents percentages of tide, fluvial and wave energy processes in Chhaosa delta. It indicates that Chhaosa delta is a tide-dominated (50.04%), fluvially influenced (30.83%) with minor wave reworking (19.13%) system

15). The ternary plots exhibit potential orders of tidal, fluvial and wave activities in the setting of twenty-two probable classification levels (Fig. 15). Sedimentary structures deposited by tide, fluvial and wave action have been estimated from the chosen sections of the study area (Fig. 14) and plotted on the ternary diagrams (Fig. 15).

Predominance of fluvial (68%) influence is well preserved in proximal parts (F1) of FA1. F1 is represented by several fluvial channels, troughs, etc. Soft sediment deformation structures like ball and pillows are indicative of fluvial flooding. The interplay of wave (19%) and tidal (13%) processes is minor in F1. F2 exhibits strong fluvial influence (56%), represented by channels, extensive sand sheets, parallel laminations and fluvial flood generated soft-sediment deformation structures. Tidal (30%) influence are indicated by flaser, wavy and lenticular bedding. Wave (14%) generated sedimentary structures are rare. Facies attributes reveal that delta plain deposit (FA1) is fluvial (62%) dominated with tide (16.5%) and wave (21.5%) influence (Fig. 15).

FA2a is considered to be deposited closer to the river mouths during progradational phases and comprises a significant amount of fluvial-generated structures. The proximal part (F3 and F4) of the delta front deposits (FA2a) exhibits strong fluvial action. F5 preserves strong tidal influence. Facies F3 exhibit strong fluvial (44%) action with tide (37%) and wave (19%) influence. Facies F4 preserves the signature of strong fluvial (40%) current, with tide (39%) and wave (21%) influences. F5 comprises primarily tide (48%) generated structures with secondary fluvial (32%) attributes and tertiary wave (20%) generated structure. Laterally extensive sand sheets, erosional bases with cross-stratifications, soft-sediment deformation structures like load cast, water escape structure and plane-parallel laminations are indicative of strong fluvial influence in the proximal part of the delta front deposit (FA2a). Abundance of sigmoidal cross-stratification, flaser beds, bidirectional cross-strata, low-angle laminations and the presence of mud drapes between stratification sets, represents overall strong tidal influence in the deposition of FA2a deposits. Wave influence in FA2a is denoted by the limited occurrences of asymmetric ripples, hummocky and swaley cross-stratifications. The interpreted proximal delta front deposits (FA2a) show a strong tidal (41.33%) and fluvial (38.67%) influence with wave (20%) activity (Fig. 15).

FA2b deposits have been inferred as tidally and wave reworked distal delta front deposits with fluvial influences (Figs. 14 and 15). Wave reworking is more pronounced in F6 and F7. F8 represents deposition by strong tidal currents. F6 exhibits dominant tide (54%) generated structures. Wave (31%) also plays an important role in the deposition of F6 with minor fluvial (15%) processes. Facies F7 preserves profuse development of tide (59%) generated sedimentary structures with significant wave (29%) and minor fluvial (12%) generated structures. Facies attributes of F8 indicate strong tidal (69%) generated structures with minor wave (19%) and fluvial (12%) influences. Tidal reworking has been delineated by the abundance of cross-stratified sandstones with mud flasers and flaser bedding. Wave-driven currents were inferred from the dominance of symmetrical ripples, oscillatory ripples, low-angle flat laminations, hummocky and swaley cross-stratification. Sedimentary structures generated by various processes indicate that FA2b bears the signature of strong tidal (61%) currents. Wave (26.33%) processes also play an important role in the deposition of FA2b with minor fluvial (12.67%) influences (Fig. 15). The top of the coarsening-upward

successions has sharp surfaces which indicate a pause in sedimentation and commencement of flooding and deposition (Fig. 15).

The strongest tidal reworking has been recognised in FA3 deposits (F9, F10 and F11). The fine-grained deposits of FA3 suggest deposition in a prodeltaic environment, with a predominance of tidal activity. Wave influences are also present in FA3 with minor fluvial activity (Figs. 14 and 15). Facies F9 reveals an indication of high tidal (72%) activity with secondary action of wave (17%) and minor fluvial (11%) generated structures. F10 represents tide (77%) generated sedimentary structures with minor wave (13%) and fluvial (10%) influences. Tidal energy (81%) is the primary process in F11 with rare or insignificant occurrences of wave (11%) and fluvial (8%). Tidal reworking has been delineated by the abundance of tidal rhythmites, flaser, wavy, and lenticular bedding, mud drapes within sets of cross-stratifications and syneresis cracks. Wave currents were also present in the prodelta deposit (FA3) as delineated by wrinkle structures, rare occurrences of asymmetrical ripples and hummocks (HCS). Fluvial-influence is rare or insignificant in the distal parts of FA3. FA3 has been designated as tide (76.67%) dominated with minor occurrences of wave (13.67%) and fluvial (9%) currents (Fig. 15).

Sequence stratigraphy

Application of sequence stratigraphy in the Chhaosa Formation was based on the mixed-energy delta depositional model facilitating palaeogeographic remodelling and identification of facies, facies relationship and facies associations distant from the depositional source. The sequence stratigraphic architecture helps to understand the process of development of different stratal stacking patterns in response to continual changing accommodation space and sediment supply in the basin. The main tools used for understanding the sequence stratigraphic architecture of the Chhaosa delta system are different lithofacies and lithofacies associations, and their spatial and temporal relationship and vertical stacking patterns of the facies associations.

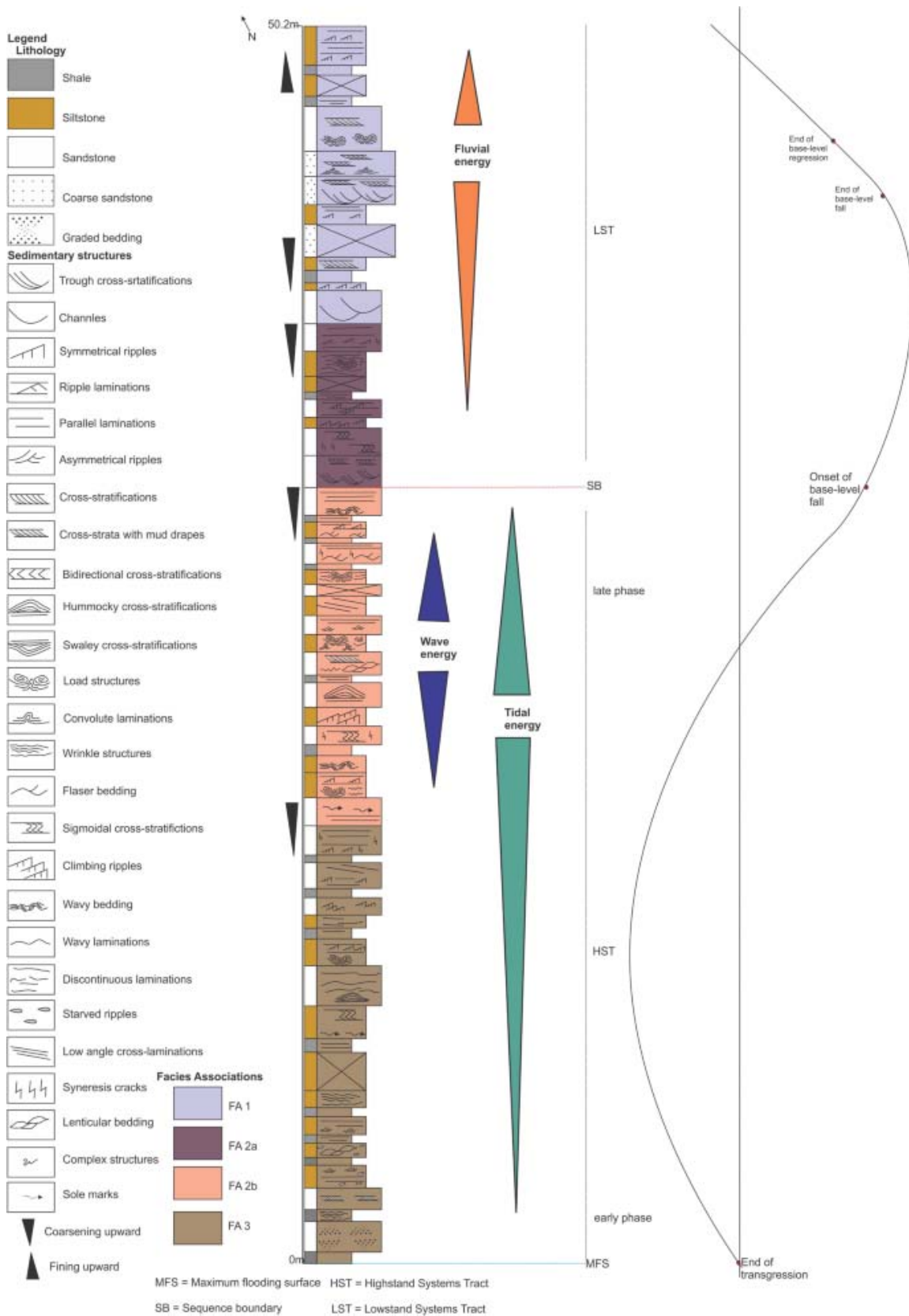


Fig. 16. Schematic log representing tide, fluvial and wave influences throughout the outcrops of the study area (FA1, FA2a, FA2b, FA3), and marking the maximum flooding surface (MFS), stages of highstand systems tract (HST), sequence boundary (SB) and lowstand systems tract (LST)





Interpreted palaeoenvironments vary from fluvial-dominated, tide and wave-influenced delta plain (FA1), to tide-dominated, fluvial and wave-influenced delta front (FA2) to tide-dominated, wave- and fluvial-influenced prodelta (FA3). The inferred delta system comprises basinward-prograding wedges, exhibiting a downlap relationship onto a mixed siliciclastic carbonate platform which itself is seen as a transgressive systems tract (TST) (Mukhopadhyay and Banerjee 2016; Mukhopadhyay and Thorie 2016; Thorie et al. 2018; Thorie et al. 2020). The calcareous marl and dark grey silty shale overlying the mixed siliciclastic carbonate platform indicates termination of transgression and thereby inferred as maximum flooding surface (MFS). The development of Chhaosa mixed-energy deltaic deposits on the top of the MFS initiates with a gradual fall of sea level along with continuous terrigenous clastic inputs, which connotes the initial stage of regression (Fig. 16). The basinward downstepping of the deltaic deposits indicates a fall in wave base in response to a gradual sea-level fall. The progradational bed sets of prodelta (FA3) to delta front (FA2) to delta plain (FA1) record the history of sea-level fluctuation. Detailed outcrop-based facies analysis and their spatial and temporal relationship and the stacking pattern of the component sequences illustrate that two different types of systems tract have been developed during the deposition of the Chhaosa mixed-energy delta succession in response to shifting of the shoreline i.e. (i) highstand systems tracts (HST) that prograde basinward with aggradational shoreline trajectory (ii) lowstand systems tracts (LST) that are represented by basinward progradation of facies belts and directly overlie the sequence boundary (Figs. 16 and 17)

Highstand systems tracts







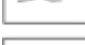



Facies associations are composed of basinward progradational wedges, downlapping over the underlying maximum flooding surface (MFS) deposits (indicated by dark grey silty shale and dolomudstone) recorded in Basantpur Formation (Mukhopadhyay and Banerjee 2016) prominently exposed in the lower part of the prodelta deposits (Fig. 16). The highstand deposits represented by the prodeltaic deposit directly overlie the mixed siliclastic inner ramp deposit of the Basantpur carbonate platform indicating that the high stand position of the sea-level prevailed from the initiation of the deposition of the inferred Chhaosa delta system. In the initial stage of highstand, the rise in relative sea-level outpaces the sedimentation rate, and the entire facies belts of FA3 and FA2b are more aggradational rather than progradational. The highstand deposits are characterized by aggradational heterolithic units FA3 (F9–F11). The occurrences of channels and troughs in the FA2b (F6–F8) might have developed due to dissection of the delta at the terminal stage of highstand (Fig. 16). Facies associations constitute basinward prograding wedges and have a downlapping relationship with fine heterolithic deposits. An increase in sediment supply during sea-level still stand condition gradually led to the culmination of progradation and ultimately deltaic sedimentation. The higher stratigraphic intervals of the successions of FA3 and FA2b display a coarsening and shallowing upward depositional trend. Hence, the prodelta and distal delta front deposits are interpreted to have deposited in highstand mixed energy condition during normal regression (Fig. 16).

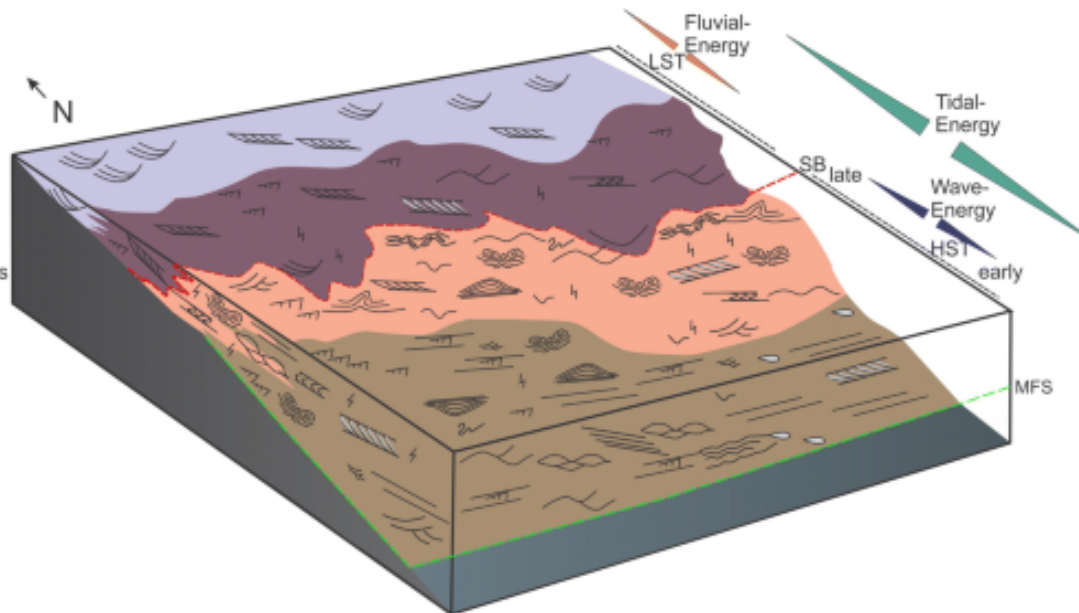
Legend

Facies Associations

-  FA 1
-  FA 2a
-  FA 2b
-  FA 3

Sedimentary structures

-  Trough cross-stratifications
-  Channels
-  Symmetrical ripples
-  Ripple laminations
-  Parallel laminations
-  Asymmetrical ripples
-  Cross-stratifications
-  Cross-strata with mud drapes
-  Bidirectional cross-stratifications
-  Sole marks







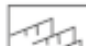
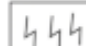










- | | | | | | |
|---|--------------------------------|--|---------------------------------|---|-----------------------------|
|  | Hummocky cross-stratifications |  | Sigmoidal cross-stratifications |  | Low angle cross-laminations |
|  | Swaley cross-stratifications |  | Climbing ripples |  | Syneresis cracks |
|  | Load structures |  | Wavy bedding |  | Lenticular bedding |
|  | Convolute laminations |  | Wavy laminations |  | Complex structures |
|  | Wrinkle structures |  | Discontinuous laminations | | |
|  | Flaser bedding |  | Starved ripples | | |
- MFS = Maximum flooding surface
HST = Highstand Systems Tract
SB = Sequence boundary
LST = Lowstand Systems Tract

Fig. 17. Schematic diagram illustrating the evolution of Proterozoic Chhaosa mixed-energy deltaic deposit in response to sea-level fluctuations (blue dotted arrows indicate different stages of HST and LST; green dotted line marks the maximum flooding surface (MFS) and red dotted line marks sequence boundary (SB). Chhaosa delta system is composed of delta plain deposit-FA1 (powder blue coloured area, top part of the diagram), proximal delta front deposits-FA2a (purple coloured area, upper middle part of the diagram), distal delta front deposits-FA2b (pink coloured area, lower middle part of the diagram) and prodelta-FA3 (brown coloured area, lower part of the diagram). Variability of tide, fluvial and wave processes has been indicated by different coloured triangles (green colour indicates tide- energy, orange colour indicates fluvial energy, and blue colour shows the wave- energy)

Sequence boundaries

The prominent and widespread erosional surfaces (along Kandaghat–Waknaghat transects) that are capped by the coarse-grained channelled sandstone deposits representing the proximal delta front deposit are demarcated as sequence boundaries as (1) these surfaces incise the entire successions of proximal delta front (FA2a) succession, (2) these surfaces cap the channelled sandstone indicating landward stepping of entire facies belts. The basal part of the proximal delta front (FA2a) is erosional to sharply based which cuts through prodelta deposit into the underlying distal delta front deposit of the Chhaosa mixed-energy delta system. The scoured base of the F5 has been identified as a sequence boundary (SB).

Lowstand systems tracts

Proximal delta front deposits (FA2a) and delta plain deposits (FA1) erosionally overlie the HST deposits of distal delta front (FA2b) and prodelta (FA3). It can be inferred that during the initiation of the evolution of the delta system regression condition of the relative sea-level prevailed and caused basinward incision which led to gradual progradation of delta. The most prominent, more-or-less continuous fluvial channels have built out strongly across the proximal part of entire deltaic succession (Figs. 16 and 17). The successions of coarse-grained deposits are interpreted as lowstand deposits. F5 and F4 can be interpreted as the early stage of LST. Fine-grained sand–silt–mud deposits overlying the fluvial channels are documented at numerous places (Fig. 16). These finer sediment deposits represent as flood plain deposits characterized by thin-bedded, fine-sandy siltstone and sandstones–mudstones (F3, F2). The late stage of LST deposit is characterized by fluvio-tidally influenced channel infillings, which (F1) ended with the initiation of braided fluvial deposits of the upper Sanjauli Formation (Mukhopadhyay et al. 2016). The fluvial deposits (channelled sandstones) with heterolithic intervals indicate interplay of tides on the fluvial deposits at the mouth of the river below the mean high tide. During the late stage of LST deposition, the fluvial deposits evolved to tidally influenced fluvial deposits, indicative of a rise in relative sea level (Fig. 16).

Depositional model

The detailed study of lithofacies and application of sequence stratigraphy facilitated to propose a paleogeographic model for the Chhaosa deltaic deposits which represents an excellent example of tide, fluvial and wave-influenced delta system (Fig. 17).

The exposures of the Chhaosa mixed-energy delta representing complex facies association (FA1) consisting of facies trends (F1 and F2) attest to the deposition of delta plain deposits (Figs. 14 and 17). The proximal part (F1) of the delta plain deposits represents distributary channels and preserves primarily fluvial-generated sedimentary structures with interplay of wave- and tide-activity (Figs. 14 and 15). The distal part (F2) of the delta plain corresponds to floodplain deposits with strong tidal, fluvial and minor wave influences (Figs. 14 and 15).

Proximal delta front deposits (FA2a) comprise facies F3, F4, F5 and exhibits common interplay of tidal, fluvial and wave activity (Figs. 14 and 17). F3 is more proximal part of FA2a and preserves signatures of strong fluvial action with tide and wave influence. Facies

attributes of F4 reveals that they have been deposited in terminal distributary channels and exhibits signature of strong fluvial, tide and wave actions (Figs. 14 and 15). F5 comprises tidally influenced mouthbar deposits and show strong tide-generated structures with interplay of fluvial and wave currents.

Deposition of F6, F7 and F8 leads to the development of distal delta front deposit (FA2b) (sharply overlying the deposits) with prominent signatures of tide, wave and fluvial influence (Figs. 14 and 15). F6 represents middle part of the delta front deposits (FA2), which is tidally influenced but wave also plays an important role with minor fluvial action. F7 and F8 represent distal part of the delta front deposit (FA2b). F7 preserves predominant tide-generated sedimentary structures with significant wave-influence and minor fluvial activity. F8 exhibits strong tidal influence with minor wave and fluvial activity.

Prodelta deposits (FA3) (interfingers with FA2b) consisting of F9, F10 and F11 exhibit clear evidence of tide- and wave-influence (Figs. 14 and 15). Facies attributes of F9 are indicative of prodeltaic origin, which preserves strong indication of tidal activity with secondary action of wave and minor fluvial activity. F10 and F11 represent the distal part of the prodelta deposits (FA3). F10 exhibit dominantly tide-generated sedimentary structures with minor wave and fluvial influence. F11 is interpreted as tidal rhythmites, which exhibit tide as the primary process with rare or insignificant occurrences of wave and fluvial processes. The percentage values of tide, fluvial and wave-generated structures delineated from eleven facies (F1-F11), measured from the chosen sections of the study area represent a tide (50.04%), fluvial (30.83%) and wave (19.13%) influenced delta system.

The reconstruction of the Chhaosa deltaic system in response to sea-level fluctuation, accommodation space and facies relationships has been determined to understand the depositional trend and history of the basin evolution in response to shoreline migration. The inferred Chhaosa mixed-energy delta exhibits an overall progradational depositional trend corresponds to normal regression. Development of highstand deposits (HST) started with the deposition of prodelta deposits (FA3) (Figs. 16 and 17). The early phase of HST deposits is represented by the deposition of F9, F10 and F11 (prodelta deposits-FA3). Distal delta front deposit (FA2b) containing F6, F7, F8 marks the late stage of HST (Figs. 16 and 17). Proximal delta front deposits (FA2a) and delta plain deposits (FA1) erosionally overlie the HST deposits of distal delta front (FA2b) and prodelta (FA3). The erosion surface at the base of F5 is interpreted as sequence boundary (Figs. 16 and 17). Proximal part of delta front (FA2a) exhibits progradational facies trends. Vertically stacked ripple laminated sandstones (F3), tabular thick-bedded sandstones (F4) and cross-bedded sandstones (F5) with fluvial and tidal indicators represent an early stage of lowstand deposit (LST) (Figs. 16 and 17). The delta plain (FA1) containing thick channel fills (F1) and thin-bedded siltstone and mud (F2) with fluvial indicators mark the late stage of LST (Figs. 16 and 17).

Comparison with modern mixed energy delta systems

The inferred Chhaosa delta system represents a classic illustration of a mixed-energy depositional environment. A comparative study of the depositional processes of recent as well as ancient deltas has been established in the present work. Few analogues of modern as well as ancient deltas have been taken into consideration for comparison as they

represent typical mixed-energy delta system to understand the control of mixed-energy processes in the ancient deltas as well as in modern deltas (Table 2). Table 2 shows that recent mixed-energy deltas are well studied and analysed rather than ancient deltas.

The Chhaosa delta system finds similarity to various mixed-energy delta systems well documented in global literature, such as the Proterozoic Reynolds Point delta (Young and Long 1977), Pennsylvanian Perrin delta (Brown Jr et al. 1990, 1973), Early Jurassic Gule Horn delta (Eide et al. 2016), Jurassic Lagas delta (Rossi and Steel 2016), Pliocene Orinoco delta (Peng et al. 2018), Holocene Mekong delta (Ta et al. 2002a, b; Xue et al. 2010) and Holocene Ganges–Brahmaputra delta (Kuehl et al. 2005) in depositional trend and nature of gradation, i.e. these deltas represent a coarsening upward subaqueous successions overlain by a fining-upward subaerial successions (delta plain deposits). But contrary to this, Table 2 shows that Pleistocene Arente delta (Fabbricatore et al. 2014) and Holocene Mitchell River delta (Massey et al. 2013; Lane et al. 2016) exhibit fining upward succession (though mixed-energy processes prevailed during their development). When lithology and depositional trend is considered, the Chhaosa represents a sand-rich delta system like recent as well as ancient deltas such as Copper River delta (Galloway 1976), Mekong delta (Ta et al 2005, 2002a, b; Xue et al. 2010) Gule Formation (Eide et al. 2016) and Lajas Formation, (Rossi and Steel 2016). Process variations in Chhaosa delta system reveal that it is tide-dominated, fluvial-influenced and wave-affected (Fig. 15), which is quite similar to Gule delta inferred by Eide et al. 2016. But Lajas delta (Rossi and Steel 2016) shows profuse development of wave-generated structures in its distal reaches, which is quite different from Chhaosa prodeltaic deposits as it records prolific development of tidal rhythmites. Fluvial energy is more pronounced in the proximal part (delta plain-FA1) and decreases towards the distal areas of the Chhaosa delta system, which resembles the depositional architecture of the delta plain and delta front deposits of Gule Formation (Eide et al. 2016) and Lajas Formation (Rossi and Steel 2016); Orinoco delta (Peng et al. 2018). But the tidal energy increases from the distal part of the delta plain (FA1) and is more pronounced in the prodelta (FA3) of the Chhaosa delta system, which is further correlative with the characteristics of the prodelta of the Gule delta (Eide et al. 2016); Orinoco delta, (Peng et al. 2018). When interplay of wave is considered, it has been observed that the Chhaosa delta system records dominant wave influence in its distal delta front (FA2b) part which is analogous to Orinoco delta (Peng et al. 2018) and Ferron delta (Li et al. 2011). The above case histories reveal that the mixed-energy processes dominantly prevailed during the sedimentation of both modern and ancient deltas and the processes of their generation are quite similar. The authors have tried to provide a brief sedimentation history of both the delta systems (Table 2).

Global case histories of ancient deltas reveal that previous workers had not concentrated much on the common interplay of the mixed-energy processes (Fluvial, wave, tide) rather they had focused on the individual depositional processes. In the present work, the Chhaosa delta has been analysed in details in terms of process variability, i.e. common interplay of fluvial, wave and tide actions and it has been inferred as a mixed-energy delta. Hence, the authors have introduced a new concept of mixed-energy processes in the present work, which led to development of a mixed-energy delta system. The 'mixed-energy' concept is not common in the global sedimentation history of the ancient deltas and the inferred Chhaosa delta system finds its uniqueness in this regard.

Table 2 Comparative study of the depositional processes of the Neoproterozoic Chhaosa delta system with recent as well as ancient deltas has been established

Sl No.	Name of delta	Age	Depositional environment	Depositional processes	Coarsening/fining upward succession	Sand/silt/ mud dominated	References
1.	Copper River delta, Cover River Basin, Alaska	Holocene	Subaerial deltaic plain; tidal lagoon complex; coastal barrier-shoreface and prodelta, tectonically uplifted, abandoned deltaic plain	Wave- and tide-dominated tidal energy with rare fluvial activity	Coarsening upward subaqueous tidal lagoon complex overlain by a fining-upward subaerial delta plain	Mud-rich	Galloway 1976
2.	Ganges–Brahmaputra delta, Bengal Basin, Bangladesh	Holocene	Upper delta plain, lower delta plain, delta front and subaqueous delta	Tide-dominated	Coarsening-upward subaqueous clinothem overlain by a fining-upward subaerial clinothem	Sand-rich	Kuehl et al. 2005 ; Peng et al. 2018
3.	Fraser, British Columbia	Holocene	Delta plain, delta front and development of many subtidal channels	Fluvial dominated, tidally influenced	--	Sand-rich	Evoy et al. 1994 ; Dashtgard et al. 2012 ; Rossi and Steel 2016
4.	Mekong, Vietnam	Holocene	Sub-aerial delta plain (including floodplain, beach ridges, marsh, or foreshore), delta front, subtidal to intertidal flat, and prodelta	Tide-dominated to mixed tide- and wave-influenced	Coarsening upward delta front overlain by a fining-upward delta plain	Sand-rich	Ta et al. 2005 , 2002 ; Rossi and Steel 2016 ; Xue et al. 2010
5.	Mitchell River delta, Karumba Basin, Gulf of Carpentaria, Australia	Holocene	Beach ridges, distributary channels, channel bars, crevasse splay and mouthbar deposits	Tide-dominated, fluvially influenced and wave affected	Fining-upward succession	Sand-rich	Massey et al. 2013 ; Lane et al. 2016
6.	Arente delta, Crati Basin (northern Calabria, southern Italy)	Pleistocene	Mouthbar sandstones, distal mouthbar conglomerates and sandstones, proximal delta front pebbly sandstones, distal delta front sandstones, wave-influenced distal delta sandstone and prodelta mudstones	Fluvial-influenced with evidence of wave reworking	Fining and thinning upward succession	Sand-rich	Fabricatore et al. 2014
7.	Orinoco delta, Manzanilla Formation, Trinidad	Pliocene	Muddy prodelta, sandier prodelta slope, outer delta-front platform, inner delta-front platform, lower delta plain	Wave influence increases from the prodelta towards the outer delta front and decreases to the inner delta front and tide influence increases from inner delta front to outer delta front and	Coarsening upward subaqueous clinothem overlain by a fining-upward subaerial clinothem.	Mud-rich	Peng et al. 2018

Table 2 (continued)

Sl No.	Name of delta	Age	Depositional environment	Depositional processes	Coarsening/fining upward succession	Sand/silt/ mud dominated	References
				decreases towards prodelta; fluvial signals were generally rare but stronger towards the upper intervals			
8.	Dir Abu Lifa Member of Qasr El-Sagha Formation, Gindi Basin(Western Desert, Egypt)	Eocene	Distributary channels, lower delta plain, delta front, Prodelta	Tide-dominated with fluvial influence and rare wave activity	Coarsening upward successions (delta front) overlain by fining upward successions (Channel-fills)	Mud-rich	Legler et al. 2013
9.	Battfjellet Formation, Spitsbergen	Eocene	Distributary channel-deposits, proximal mouthbar deposits, distal mouthbar deposits, prodelta slope	Wave-dominated, fluvial and tide influenced	Coarsening upward successions of proximal and distal mouthbar deposits are overlain by fining upward channel-fill deposits	Sand-rich	Plink-Björklund 2005
10.	Ferron Sandstone Member ('Notom' delta), Mancos Shale Formation, Utah, USA	Cretaceous (Turonian)	Proximal delta front; distal delta front, prodelta, distributary channel and mouthbar	Wave and river dominated	Coarsening upward successions (distal lower shoreface to upper shoreface) passing into a fine grained succession (from upper shoreface to beach)	Sand-rich	Li et al. 2011
11.	Panther Tongue delta, Star point Formation central Utah, USA	Cretaceous	Terminal distributary channel, channel mouth, proximal delta-front and distal delta-front	River-dominated with seasonal wave- and storm influence	Coarsening-and thickening- upward succession	Sand-rich	Olariu et al. 2005 ; Olariu and Bhattacharya 2006 ; Olariu et al. 2010
12.	Lajas Formation, Neuquén Basin, Argentina	Jurassic	Coastal plain, Delta Front and Subaqueous Platform, Prodelta and Offshore, Tidal Inlet and Estuary	Wave generated structures were more pronounced in the distal part of the delta and whereas river influence were stronger towards the proximal parts. Tidal influence was stronger in the delta front and subaqueous platform areas	Coarsening- upward delta front and subaqueous platform overlain by fining upward sub subaerial coastal plains	Sand-rich	Rossi and Steel 2016
13.	Gule Horn Formation, Jameson Land, Greenland	Early Jurassic	Delta plain, delta front, prodelta	Tide-influenced with strong fluvial influence and minor wave activity	Coarsening upward tidal bars of delta front deposits are overlain by fining upward distributary channels of delta plain deposits	Sand-rich	Eide et al. 2016
14.	Perrin Delta, Canyon Group in North-Central Texas	Pennsylvanian	Delta plain, distributary channels, proximal delta front, distal delta front, Prodelta	River and wave dominated	Coarsening upward sequences	Sand-rich	Brown et al 1990 , 1973

Table 2 (continued)

Sl No.	Name of delta	Age	Depositional environment	Depositional processes	Coarsening/fining upward succession	Sand/silt/mud dominated	References
15.	Chhaosa Formation, Simla group, Lesser Himalaya, India	Neoproterozoic	Delta plain (FA1), proximal delta front (FA2a), distal delta front (FA2b) and prodelta (FA3)	Dominance of tidal currents with fluvial- and wave- influence	Coarsening-upward front deposit (FA3 and FA2) overlain by fining upward delta plain deposit (FA1)	Sand-rich	Kumar and Brookfield 1987, Mukhopadhyay et al. 2016.
16.	Morro do Chapéu Formation, Chapada Diamantina Basin, Espinhaço supergroup–Ne/Brazil	Mesoproterozoic	Wave-reworked fan-delta	Mixed wave-tide--dominated	Coarsening upward successions	Sand-rich	De Souza et al. 2019
17.	Braid delta in the Næringselva Member, Båsnæringen Formation of the Barents Sea Group, Varanger Peninsula, northern Norway	Proterozoic	Prodelta slope, delta-front sandstones	Flash-flood dominated	Coarsening upward successions	Mud-rich	Hjellbakk 1997
18.	Reynolds Point Formation, Shaler Group Victoria Island, Canada	Proterozoic	Prodelta and distal delta slope deposits	Tide-influenced	Coarsening upward successions (prodelta and distal delta slope) overlain by fining upward distributary bays	Sand-rich	Young and Long 1977

Palaeotectonic significance

In ancient and modern coastal clastic systems, mixed-energy deltas reflect rapid variations in the depositional process in space through time. These variations in energy condition and depositional setup throughout different time frames are usually associated with base-level fluctuations accompanied by the development of deltas and estuaries (Dalrymple et al. 1992; Buatois et al. 2011; Ichaso and Dalrymple 2014; Rossi and Steel 2016; Peng et al. 2018). Global sedimentological history of mixed-energy deltas reveals that changes in process regime occur within a short span of time due to local sedimentary processes and tectonic processes (Ta et al. 2002a, b; Olariu 2014; Rossi and Steel 2016). These changes are crucial, due to their influence on sediment pattern, distribution of facies attributes and also delta morphology. The Simla Basin, considered a typical rifted basin by Kumar and Brookfield 1987 represents a suitable example in this regard. It can be assumed that due to rifting, the palaeotectonic condition of the Simla Basin, provides favourable conditions for the generation of mixed-energy deltaic deposits. Similar ancient basins bearing mixed-energy deltaic deposits were also recorded by other workers (Massey et al. 2013; Lane et al. 2016; Rossi and Steel 2016; Peng et al. 2018). Rifting introduced extra complexity to the evolution of the Chhaosa coastal successions. The rifted basin increased in depth, length and gradually infilled with sediment, with mixed-energy conditions marked by rapid lateral and vertical facies variations in the Chhaosa coastal deposits. The abundance of load structures in several stratigraphic horizons in the Chhaosa Formation indicates rapid deposition before auto-compaction probably due to faulting (Kumar and Brookfield 1987). Kumar and Brookfield (1987) speculated that the deposition of sediments in the Simla Group took place within a short period. Hence, it can be assumed that the rapid facies variation in response to sea-level fluctuation occurred due to continuous subsidence of the basin related to basin marginal faulting during rift extension. The agglomeration of displacement due to the repetitive occurrence of faulting caused by rifting generated greater accommodation and thicker regressive deposits.

In spite of being an ancient deltaic system, the Chhaosa delta provides an excellent example in this regard where all these process fluctuations can be prominently observed (Fig. 17).

Conclusions

The Chhaosa Formation has developed during aggradation and progradation, superimposed on longer-term periods of progradation. Traverses along chosen transects unravel the different facies associations of the Chhaosa Formation.

The lateral and vertical facies variations found in the middle-upper part of the Chhaosa Formation reveal that the depositional environment of a sand-rich mixed-energy delta system with delta plain (FA1) proximal delta front (FA2a), distal delta front (FA2b) and prodelta (FA3) representing aggradational–progradational stacking pattern. The delta system was predominantly medium- to fine-grained.

Fluvial currents are stronger in more proximal areas (FA1). The sediments of proximal delta front deposits (FA2a) were re-worked by tidal and wave activity. Distal delta front (FA2b)

comprises tide-generated structures with a significant amount of wave activity. Prodelta (FA3) represents strong tidal activity with a minor wave and fluvial influences.

Overall, the Chhaosa delta is strongly influenced by tidal energy, which is characterized by (i) heterolithic bedding; (ii) flaser, lenticular and wavy bedding; (iii) mud flasers along with forests; (iv) sigmoidal cross-bedding; (v) bidirectional cross-stratification; and (vi) tidal rhythmites. Fluvial processes were infused with the other processes, but they are distinctively noticeable from (i) vertically stacked fluvial channels; (ii) trough cross-stratifications; (iii) coarse grain size; and (iv) extensive sand-sheets. Signatures of wave activities have been indicated by the following features: (i) swales and hummocky cross-stratifications; (ii) low-angle lamination; (iii) wavy bedding; (iv) wave ripples; (v) oscillatory ripples; (vi) current ripples; and (vii) wrinkle structure.

Profuse development of fluvial generated structures towards the proximal part of the successions with decreased wave action indicates progradational trend of the delta system.

The coastal process classification ternary plots reveal that the Chhaosa deltaic succession is strongly influenced by reworking of tide, fluvial and wave energies and is very distinctive from typical coarsening upward river-dominated, wave-dominated and tide-dominated deltas.

A comparison between the studied delta system and other delta systems has been illustrated to understand the control of fluvial, wave and tidal energy in the ancient deltas as well as in modern deltas. The 'mixed-energy' concept is not common in the global sedimentation history of the ancient deltas, as the previous workers mainly focuses on classic river-, tide-, wave-dominated models. The inferred Chhaosa delta system finds its uniqueness in this regard.

Acknowledgements

We appreciate the infrastructural support given by the university authorities. Our appreciation goes to Prof. Ravindra Kumar (retired) of the Department of Geology, Panjab University, Chandigarh, India, for his contribution towards this research work. We also thank Sushil Thakur for field assistance.

References

Ahmed S, Bhattacharya JP, Garza DE, Li Y (2014) Facies architecture and stratigraphic evolution of a river-dominated delta front, Turonian Ferron sandstone, Utah, U.S.A. *J Sediment Res* 84(2):97–121

Ainsworth RB, Vakarelov BK, Nanson RA (2011) Dynamic spatial and temporal prediction of changes in depositional processes on clastic shorelines: toward improved subsurface uncertainty reduction and management. *AAPG Bull* 95(2):267–297

Ainsworth RBB, Vakarelov K, MacEachern JA, Nanson RA, Lane TI, Rarity F and Dashtgard SE (2016) Process-driven architectural variability in mouth-bar deposits: A case study from a mixed-process mouth-bar complex, Drumheller, Alberta, Canada. *J Sediment Res* 86(5) 512–541. <https://doi.org/10.2110/jsr.2016.23>

Allen JRL (1980) Sand waves: a model of origin and internal structure. *Sediment Geol* 26(4):281–328

Allen PA, Honewood P (1984) Evolution and mechanics of a Miocene tidal sandwave. *Sedimentology* 31:63–81

Anell I, Zuchuat V, Röhnert AD, Smyrak-Sikora A, Lord G, Maher H, Midtkandal I, Ogata K, Olausson S, Osmundsen PT, Braathen A (2020) Tidal amplification and along-strike process variability in a mixed-energy paralic system prograding onto a low accommodation shelf, Edgeøya, Svalbard. *Basin Res*

Basilici G, de Luca PHV, Poiré DG (2012) Hummocky cross-stratification-like structures and combined-flow ripples in the Punta Negra Formation (Lower-Middle Devonian, Argentine Precordillera): a turbiditic deep-water or storm-dominated prodelta inner-shelf system? *Sediment Geol* 267–268:73–92

Bhattacharya J, Walker RG (1991) River and wave-dominated depositional systems of the Upper Cretaceous Dunvegan Formation, northwestern Alberta. *Bull Can Petrol Geol* 39:165–191

Bowman AP, Johnson HD (2014) Storm-dominated shelf-edge delta successions in a high accommodation setting: The palaeo-Orinoco Delta (Mayaro Formation), Columbus Basin, South-East Trinidad. *Sedimentology* 61:792–835

Brown LF Jr, Solis-Iriarte RF, and Johns DA (1990) Regional depositional systems tracts, paleogeography, and sequence stratigraphy, Upper Pennsylvanian and Lower Permian Strata, North- and West-Central Texas: Texas Bureau of Economic Geology, Reports of Investigations 197: pp116

Brown LF, Cleaves JR, and Erxleben AW (1973) Pennsylvanian depositional systems in North-Central Texas—a guide for interpreting terrigenous clastic facies in a cratonic basin: Texas Bureau of Economic Geology, Guidebook 14: pp122

Buatois LA, Mángano MG (2003) Sedimentary facies, depositional evolution of the Upper Cambrian–Lower Ordovician Santa Rosita formation in northwest Argentina. *J S Am Earth Sci* 16(5):343–363

Buatois LA, Saccavino LL and Zavala C (2011) Ichnologic signatures of hyperpycnal-flow deposits in Cretaceous river-dominated deltas, Austral Basin, southern Argentina. In: Slatt

RM and Zavala C (eds), sediment transfer from shelf to deep water – revisiting the delivery system. AAPG Stud Geol 61

Buatois LA, Santiago N, Herrera M, Plink-Björklund P, Steel R, Espin M, Parra K (2012) Sedimentological and ichnological signatures of changes in wave, river and tidal influence along a Neogene tropical deltaic shoreline. *Sedimentology* 59(5):1568–1612

Carmona N, Buatois L, Ponce J, Mangano M (2009) Ichnology and sedimentology of a tide-influenced delta, Lower Miocene Chenque Formation, Patagonia, Argentina: trace-fossil distribution and response to environmental stresses. *Palaeogeogr Palaeoclimatol Palaeoecol* 273:75–86

Chen L, Lu YC, Wu JY, Xing FC, Liu L, Ma YQ, Rao D, Peng L (2015) Sedimentary facies and depositional model of shallow water delta dominated by fluvial for Chang 8 oil-bearing group of Yanchang Formation in southwestern Ordos Basin, China. *J Cent South Univ* 22(12):4749–4763

Choi K (2010) Rhythmic climbing-ripple cross-lamination in inclined heterolithic stratification (IHS) of a macrotidal estuarine channel, Gomso Bay, west coast of Korea. *J Sediment Res* 80:550–561

Choi K (2011) Tidal rhythmites in a mixed-energy, macrotidal estuarine channel, Gomso Bay, west coast of Korea. *Mar Geol* 280:105–115

Clifton HE (2006) A reexamination of facies models for clastic shorelines. In: Posamentier HW, Walker RG (eds) *Facies models revisited*, vol 84. SEPM Spec Publ, pp 293–337

Cummings DI, Arnott RWC, Hart BS (2006) Tidal signatures in a shelfmargin delta. *Geology* 34:249–225

Dalrymple RW, Zaitlin BA, Boyd R (1992) Estuarine facies models; conceptual basis and stratigraphic implications. *J Sediment Res* 62(6):1130–1146

Dalrymple RW, Baker EK, Harris PT and Hughes MG (2003) Sedimentology and stratigraphy of a tide-dominated, foreland-basin delta (Fly River, Papua New Guinea). In: Sidi FH, Nummedal D, Imbert P, Darman Hand Posamentier HW (eds) *Tropical deltas of Southeast Asia-Sedimentology, Stratigraphy, and Petroleum Geology*. SEPM Spec Publ 76: 147–173

Dasgupta P (2005) Facies pattern of the middle Permian Barren Measures Formation, Jharia basin, India: the sedimentary response to basin tectonics. *J Earth Syst Sci* 114(3):287–302

Dashtgard S, Venditti J, Hill P, Sisulak C, Johnson S, La Croix A (2012) Sedimentation across the tidal fluvial transition in the lower Fraser River, Canada. *Sed Rec* 10:4–9

De Souza EG, Scherer CMS, dos Reis AD, Bállico MB, Ferronato JPF, Bofill LM, Kifumbi C (2019) Sequence stratigraphy of the mixed wave-tidal-dominated mesoproterozoic sedimentary succession in Chapada Diamantina Basin, Espinhaço Supergroup–Ne/Brazil. *Precambrian Res* 327:103–120

- Dumas S, Arnott RWC, Southard JB (2005) Experiments on oscillatory flow and combined-flow bed forms: implications for interpreting parts of the shallow marine sedimentary record. *J Sediment Res* 75:501–513
- Eide CH, Howell JA, Buckley SJ, Martinius AW, Oftedal BT, Henstra GA (2016) Facies model for a coarse-grained, tide-influenced delta: Gule Horn Formation (Early Jurassic), Jameson Land, Greenland. *Sedimentology* 63(6):1474–1506
- Eilertsen RS, Corner GD, Aasheim O, Hansen L (2011) Facies characteristics and architecture related to palaeodepth of Holocene fjord–delta sediments. *Sedimentology* 58:1784–1809
- Eltayib SHMA, Al-Imam OAO, Adam HJ, Salim MA (2018) Sedimentary environments and lithofacies distribution of Upper Shendi Formation, Central Sudan. *Int J Geol Agric Environ Sci* 6(4)
- Eriksson PG, Condie KC, Tirsgaard H, Mueller WU, Altermann W, Miall AD, Aspler LB, Catuneanu O, Chiarenzelli JR (1998) Precambrian clastic sedimentation systems. *Sediment Geol* 120:5–53
- Evoy RW, Moslow TF, Kostaschuk RA, Luternauer JL (1994) Origin and variability of sedimentary facies of the Fraser River delta foreslope, British Columbia. *Mar Geol* 118:49–60
- Fabbricatore D, Robustelli G, Muto F (2014) Facies analysis and depositional architecture of shelf-type deltas in the Crati Basin (Calabrian Arc, south Italy). *Ital J Geosci* 133:131–148
- Feldman HR, Fabijanic JM, Faulkner BL, Rudolph KW (2014) Lithofacies, parasequence stacking, and depositional architecture of wave- to tide-dominated shorelines in the Frontier Formation, western Wyoming, USA. *J Sediment Res* 84:694–717
- Fernández LP, Águeda JA, Colmenero JR, Salvador CI, Barba P (1988) A coal-bearing fan-delta complex in the Westphalian D of the Central Coal Basin, Cantabrian Mountains northwestern Spain: implications for the recognition of humid-type fan deltas. In: Nemeč W, Steel RJ (eds) *Fan deltas: sedimentology and tectonic settings*. Blackie and Son, London, pp 286–302
- Frank W, Bhargava ON, Miller CH, Banerjee DM (2001) A review of the Proterozoic in the Himalaya and the northern Indian Shield. *J. Asian Earth Sc. Special Abstract Issue, 16th Himalaya–Karakoram–Tibet Workshop* 19(3 A) 18
- Galloway WE (1975) Process framework for describing the morphologic and stratigraphic evolution of deltaic depositional systems. In: Broussard M (ed) *Deltas: models for exploration*: Houston. Houston Geol Soc, Texas, pp 87–98
- Galloway WE (1976) Sediments and stratigraphic framework of the Copper River fan-delta, Alaska. *J Sediment Res* 46(3):726–737

- Gani MR, Bhattacharya JP (2007) Basic building blocks and process variability of a Cretaceous delta: internal facies architecture reveals a more dynamic interaction of river, wave, and tidal processes than is indicated by external shape. *J Sediment Res* 77:284–302
- Geological Survey of India (1976) *Memoirs of the geological survey of India* 106: Part 1
- Gugliotta M, Kurcinka CE, Dalrymple RW, Flint SS, Hodgson DM (2016) Decoupling seasonal fluctuations in fluvial discharge from the tidal signature in ancient deltaic deposits: an example from the Neuquén Basin, Argentina. *J Geol Soc* 173(1):94–107
- Hampton BA, Horton BK (2007) Sheet flow fluvial processes in a rapidly subsiding basin, Altiplano plateau, Bolivia. *Sedimentology* 54(5):1121–1148
- Hjellbakk A (1997) Facies and fluvial architecture of a high-energy braided river: the Upper Proterozoic Seglommen Member, Varanger Peninsula, northern Norway. *Sediment Geol* 114:131–161
- Horne JC, Ferm JC, Caruccio FT, Baganz BP (1978) Depositional models in coal exploration and mine planning in Appalachian region. *AAPG Bull* 62:2379–2411
- Ichaso AA, Dalrymple RW (2014) Eustatic, tectonic and climatic controls on an early syn-rift mixed-energy delta, Tilje Formation (early Jurassic, Smørbukk Field, offshore mid-Norway). In: Martinius AW, Ravnås R, Howell JA, Steel RJ, Wonham JP (eds) *From depositional systems to sedimentary successions on the Norwegian Continental Shelf*, vol 46. *Int Assoc Sedimentol Spec Publ*, pp 339–388
- Jaiswal S, Bhattacharya B (2018) Characterization of middle Eocene tide-influenced delta: a study from core samples of Hazad Member, Ankleshwar Formation, South Cambay Basin, India. *J Earth Syst Sci* 127:65. <https://doi.org/10.1007/s12040-018-0966-8>
- Johnson HD, Baldwin CT (1996) Shallow clastic seas. In: Reading HG (ed) *Sedimentary environments: processes, facies and stratigraphy*. Blackwell, Oxford, pp 232–280
- Johnson CL, Stright L, Purcell R, and Durkin P (2016) Stratigraphic evolution of an estuarine fill succession and the reservoir characterization of inclined heterolithic strata, Cretaceous of southern Utah, USA, in Hampson GJ, Reynolds AD, Kostic B and Wells MR (eds) *Sedimentology of Paralic Reservoirs: Recent Advances*: *Geol Soc London Spec Publ* 444:pp 251–286
- Khanam F, Rahman MJJ, Alam MM, Abdullah R (2017) Facies characterization of the Surma Group (Miocene) sediments from Jalalabad gas field, Sylhet Trough, Bangladesh: study from cores and wireline log. *J Geol Soc India* 89:155–164
- Kiwango AS, Mishra D (2020) Sedimentology and paleocurrent study of the Early Triassic Rocks in the Ruhuhu Basin, SW Tanzania. *Tanzania J Sci* 46(2):383–396

Kneller BC (1995) Beyond the turbidite paradigm: physical models for deposition of turbidites and their implications for reservoir prediction. In: Hartley AJ, Prosser DJ (eds) *Characterization of Deep Marine Clastic Systems: Geol Soc Lond, Spec Publ, vol 94*, pp 31–49

Kuehl SA, Allison MA, Goodbred SL, Kudrass H (2005) The Ganges– Brahmaputra Delta, In: Gioson L, and Bhattacharya JP (eds) *river deltas: concepts, models and examples: SEPM. Special Publication 83:413–434*

Kumar R, Brookfield ME (1987) Sedimentary environments of the Simla Group (Upper Precambrian), Lesser Himalaya, and their paleotectonic significance. *Sediment Geol* 52(1-2):27–43

Kundu A, Goswami B, Eriksson PG, Chakraborty A (2011) Palaeoseismicity in relation to basin tectonics as revealed from soft-sediment deformation structures of the Lower Triassic Panchet formation, Raniganj basin (Damodar valley), eastern India. *J Earth Syst Sci* 120:167–181

Kvale EP (2003) Tides and tidal rhythmites. In: Middleton GV (ed) *Encyclopedia of sediments and sedimentary rocks*. Kluwer Academic, Dordrecht, pp 741–744

Kvale EP, Archer AW, Johnson HR (1989) Daily, monthly, and yearly tidal cycles within laminated siltstones of the Mansfield Formation (Pennsylvanian) of Indiana. *Geology* 17:365–368

Lane TI, Nanson RA, Vakarelov BK, Ainsworth RB, Dashtgard SS (2016) Evolution and architectural styles of a forced-regressive Holocene delta and megafan, Mitchell River, Gulf of Carpentaria, Australia. In: Hampson GJ, Reynolds AD, Kostic B, Wells MR (eds) *Sedimentology of paralic reservoirs: recent advances*. Geol Soc London Spec Publ, p 444. <https://doi.org/10.1144/SP444.9>

Lee K, Zeng X, Mcmechan GA, Howell CD, Bhattacharya JP, Marcy F and Olariu C (2005) A ground-penetrating radar survey of a delta-front reservoir analog in the Wall Creek Member, Frontier Formation, Wyoming: *Americ Assoc of Petrol Geol Bull* 89: 1139–1155

Legler B, Johnson HD, Hampson GJ, Massart BYG, Jackson CA-L, Jackson MD, Ael-Barkooky, Ravnas R (2013) Facies model of a fine-grained, tide-dominated delta: Lower Dir Abu Lifa Member (Eocene), Western Desert, Egypt. *Sediment* 60(5):1313–1356

Legler B, Hampson GJ, Jackson CA, Johnson HD, Massart BYG, Sarginson M, Ravnas R (2014) Facies relationships and stratigraphic architecture of distal, mixed tide- and wave-influenced deltaic deposits: Lower Segeo Sandstone, Western Colorado, U.S.A. *J Sediment Res* 84:605–625

Leren BLS, Howell J, Enge H, Martinius AW (2010) Controls on stratigraphic architecture in contemporaneous delta systems from the Eocene Roda Sandstone, Tremp-Graus Basin, northern Spain. *Sediment Geol* 229(1-2):9–40

- Li W, Bhattacharya JP, Zhu Y, Garza D, Blankenship E (2011) Evaluating delta asymmetry using 3D facies architecture and ichnological analysis, Ferron Notom Delta, Capital Reef Utah, USA. *Sedimentology* 58:478–507
- Li Z, Bhattacharya J, Schieber J (2015) Evaluating along-strike variation using thin-bedded facies analysis, upper cretaceous Ferron Notom delta, Utah. *Sedimentology* 62:2060–2089
- MacEachern JA, Pemberton SG (1994) Ichnological aspects of incised-valley fill systems from the Viking Formation of the western Canada sedimentary basin, Alberta, Canada. In: Dalrymple RW, Boyd R, Zaitlin BA (eds) *Incised valley systems: origins and sedimentary sequences*, vol 51. Soc of Econo Paleont and Mineral, Spec Publ, pp 129–157
- Magalhães AJC, Scherer CMS, Raja Gabaglia GP, Catuneanu O (2015) Mesoproterozoic delta systems of the Açuruá Formation, Chapada Diamantina, Brazil. *Precambrian Res* 257:1–21
- Mángano MG, Buatois LA (2004) Ichnology of Carboniferous tide-influenced environments and tidal flat variability in the North American Midcontinent. In: McIlroy D (ed) *The application of ichnology to palaeoenvironmental and stratigraphic analysis*, vol 228. Geol Soc London Spec Publ, pp 157–178
- Massey TA, Fernie AJ, Ainsworth RB, Nanson RA, Vakarelov BK (2013) Detailed mapping, three-dimensional modelling and upscaling of a mixed-influence delta system, Mitchell River delta, Gulf of Carpentaria, Australia. In: Martinius AW, Howell JA, Good TR (eds) *Sediment[1]Body Geometry and Heterogeneity: Analogue Studies for Modelling the Subsurface*. Geological Society, London, Spec Publ, p 387. <https://doi.org/10.1144/SP387.4>
- Mazumder R, Arima M (2005) Tidal rhythmites and their implications. *Earth–Sci Rev* 69(1–2):79–95
- McKenzie NR, Hughes NC, Myrow PM, Xiao S, Sharma M (2011) Correlation of precambrian-cambrian sedimentary success across northern India and the utility of isotopic signatures of Himalayan lithotectonic zones. *Earth Planet Sci Lett* 312:471–483
- Medlicott HB (1864) On the geological structures and relations of the southern portion of the Himalayan ranges between the rivers Ganges and Ravee. *Mem Geol Sure India* 3(2):1–212
- Miall AD (1996) *The geology of fluvial deposits: Berlin sedimentary facies, basin analysis, and petroleum geology*. Springer-Verlag, Heidelberg, p 582
- Mode AW, Ekwenye OC, Oha IA, Onah FC (2018) Facies analysis and ichnology of a prograding river-dominated and wave-influenced deltaic deposit: the Nkporo Formation in the Itigidi-Ediba region of the Afikpo Sub-basin, south-eastern Nigeria. *J Afr Earth Sci* 147:152–168
- Mukhopadhyay A, Banerjee T (2016) Stromatolites: a guideline for development of a carbonate ramp, Basantpur Formation, Neoproterozoic Simla Group in Lesser Himalaya, India. *Arab J Geosci* 9:521

- Mukhopadhyay A, Thorie A (2016) Comparative study of two relatives, MISS and stromatolites: example from the Proterozoic Kuniyar Formation, Simla Group, Lesser Himalaya. *Arab J Geosci* 9(8):521
- Mukhopadhyay A, Mazumdar P, Van Loon AJ (2016) A new 'superassemblage' model explaining proximal-to-distal and lateral facies changes in fluvial environments, based on the Proterozoic Sanjauli Formation (Lesser Himalaya, India). *J Palaeogeogr* 5(4):391–408
- Mulder T, Syvitski JPM, Migeon S, Faugères J-C, Savoye B (2003) Marine hyperpycnal flows: initiation, behavior and related deposits: a review. *Mar Pet Geol* 20:861–882
- Mutti E, Tinterri R, Benevelli G, di Biase D, Cavanna G (2003) Deltaic, mixed and turbidite sedimentation of ancient foreland basins. *Mar Pet Geol* 20(6–8):733–755
- O'Connell B, Dorsey RJ, Humphreys ED (2017) Tidal rhythmites in the southern Bouse Formation as evidence for post-Miocene uplift of the lower Colorado River corridor. *Geology* 45:99–102
- Olariu C (2014) Autogenic process change in modern deltas: lessons for the ancient. In: Martinius AW, Ravnås R, Howell JA, Steel RJ, Wonham JP (eds) *From depositional systems to sedimentary successions on the Norwegian continental margin*, vol 46. IAS Spec Publ, pp 149–166
- Olariu C, Bhattacharya JP (2006) Terminal distributary channels and delta front architecture of river dominated delta systems. *J Sediment Res* 76(2):212–233
- Olariu C, Bhattacharya JP, Xu X, Aiken CLV, Zeng X, Mcmechan GA (2005) Integrated study of ancient delta front deposits, using outcrop, ground penetrating radar and three dimension photorealistic data: cretaceous Panther Tongue sandstone, Utah. In: Giosan L, Bhattacharya JP (eds) *River Deltas: Concepts, Models, Examples*, vol 83. SEPM Spec Publ, pp 155–178
- Olariu C, Steel RJ, Petter AL (2010) Delta-front hyperpycnal bed geometry and implications for reservoir modeling: cretaceous Panther Tongue delta. *Book Cliffs, Utah. AAPG Bull* 94(6):819–845
- Olariu MI, Carvajal C, Olariu C, Steel RJ (2012) Deltaic process and architectural evolution during cross-shelf transits, Maastrichtian Fox Hills Formation, Washakie Basin. *Wyoming. AAPG Bull* 96(10):1931–1956. <https://doi.org/10.1306/03261211119>
- Peng Y, Steel RJ, Rossi VM, Olariu C (2018) Mixed-energy process interactions read from a compound-clinoform delta (paleo-Orinoco Delta, Trinidad): preservation of river and tide signals by mud-induced wave damping. *J Sediment Res* 88(1):75–90
- Peng Y, Steel RJ, Olariu C, Li S (2020) Rapid subsidence and preservation of fluvial signals in an otherwise wave-reworked delta front succession: early-mid Pliocene Orinoco continental margin growth, SE Trinidad. *Sediment Geol* 395:105555

- Plink-Björklund P (2005) Stacked fluvial and tide-dominated estuarine deposits in high frequency (fourth-order) sequences of the Eocene Central Basin, Spitsbergen. *Sedimentology* 52(2):391–428
- Plink-Björklund P (2020) Shallow-water deltaic clinoforms and process regime. *Basin Res* 32(2):251–262
- Plint AG, Wadsworth JA (2003) Sedimentology and palaeogeomorphology of four large valley systems incising delta plains, western Canada Foreland Basin: implications for mid-Cretaceous sea-level changes. *Sedimentology* 50(6):1147–1186
- Plummer PS, Gostin VA (1981) Shrinkage cracks: desiccation or synaeresis. *J Sediment Petrol* 51:1147–1156
- Puigdomenech CG, Carvalho B, Paim PSG, Faccini UF (2014) Lowstand turbidites and delta systems of the Itararé Group in the Vidal Ramos region (SC), southern Brazil. *Braz J Geol* 44(4):529–544
- Rahman MJJ, Faupl P, Alam MM (2009) Depositional facies of the subsurface Neogene Surma group in the Sylhet trough of the Bengal Basin, Bangladesh: record of tidal sedimentation. *Int J Earth Sci* 98:1971–1980
- Rana N, Prakash Sati S, Sundriyal Y, Juyal N (2016) Genesis and implication of soft sediment deformation structures in high energy fluvial deposits of the Alaknanda valley, Garhwal Himalaya, India. *Sediment Geol* 344:263–276
- Reineck HE, Singh IB (1980) Depositional sedimentary environments: with reference to terrigenous clastics. Springer-Verlag, Berlin Heidelberg, p 551
- Reineck HE, Wunderlich F (1968) Classification and origin of flaser and lenticular bedding. *Sedimentology* 11(1-2):99–104
- Rossi VM, Steel RJ (2016) The role of tidal, wave and river currents in the evolution of mixed-energy deltas: example from the Lajas Formation (Argentina). *Sedimentology* 63(4):824–864
- Saitoh Y, Masuda F (2013) Spatial change of grading pattern of subaqueous flood deposits in Lake Shinji, Japan. *J Sediment Res* 83:221–233
- Samanta P, Mukhopadhyay S, Eriksson PG (2016) Forced regressive wedge in the Mesoproterozoic Koldaha shale, Vindhyan basin, Son Valley, central India. *Mar Petrol Geol* 71:329–343. <https://doi.org/10.1016/j.marpetgeo.2016.01.001>
- Sarkar S, Bose PK, Samanta P, Sengupta P, Eriksson PG (2008) Microbial mat mediated structures in the Ediacaran Sonia Sandstone, Rajasthan, India, and their implications for Proterozoic sedimentation. *Precambrian Res* 162(1-2):248–263

- Sarkar S, Banerjee S, Samanta P, Chakraborty PP, Mukhopadhyay S, Singh AK (2014) Microbial mat records in siliciclastic rocks: examples from Four Indian Proterozoic basins and their modern equivalents in Gulf of Cambay. *J Asian Earth Sci* 91:362–377
- Shanmugam G (2017) Global case studies of soft-sediment deformation structures (SSDS): definitions, classifications, advances, origins, and problems. *J Palaeogeogr* 6(4):251–320
- Shukla UK, Bachmann GH, Singh IB (2010) Facies architecture of the Stuttgart Formation (Schilfsandstein, Upper Triassic), Central Germany, and its comparison with modern Ganga system, India. *Palaeogeogr Palaeoclimatol Palaeoecol* 297:110–128
- Skelly RL, Bristow CS, Ethridge FG (2003) Architecture of channel-belt deposits in an aggrading shallow sandbed braided river: the lower Niobrara River, northeast Nebraska. *Sediment Geol* 158(3-4):249–270
- Smyrak-Sikora A, Osmundsen PT, Braathen A, Ogata K, Anell I, Mulrooney MJ, and Zuchuat V (2019) Architecture of growth basins in a tidally influenced, prodelta to delta front setting: the Triassic succession of Kvalpynten, East Svalbard. *Basin Res*
- Spalletti LA, Piñol FC (2005) From alluvial fan to playa: an upper jurassic ephemeral fluvial system, Neuquén Basin, Argentina. *Gondwana Res* 8(3):363–383
- Ta TKO, Nguyen VL, Tateishi M, Kobayashi I, Saito Y, Nakamura T (2002a) Sediment facies and Late Holocene progradation of the Mekong River Delta in Bentre Province, southern Vietnam: an example of evolution from a tide-dominated to a tide- and wave- dominated delta. *Sediment Geol* 152(3-4):313–325
- Ta TKO, Nguyen VL, Tateishi M, Kobayashi I, Tanabe S, Saito Y (2002b) Holocene delta evolution and sediment discharge of the Mekong River, southern Vietnam. *Quat Sci Rev* 21(16-17):1807–1819
- Ta TKO, Nguyen VL, Tateishi M, Kobayashi I, Saito Y (2005) Holocene delta evolution and depositional models of the Mekong River Delta, Southern Vietnam, River Deltas — concepts, models, and examples. *SEPM*, pp 453–466
- Tanner LH, Lucas SG (2010) Deposition and deformation of fluvial–lacustrine sediments of the Upper Triassic–Lower Jurassic Whitmore Point Member, Moenave Formation, northern Arizona. *Sediment Geol* 223(1):180–191
- Taral S, Chakraborty T (2018) Deltaic coastline of the Siwalik (Neogene) foreland basin: evidences from the Gish River section, Darjeeling Himalaya. *Geol J* 53(1):203–229
- Thorie A, Mukhopadhyay A, Banerjee T, Mazumdar P (2018) Giant ooids in a Neoproterozoic carbonate shelf, Simla Group, Lesser Himalaya, India: an analogue related to Neoproterozoic glacial deposits. *Mar Pet Geol*:582–606

Thorie A, Mukhopadhyay A, Mazumdar P, Banerjee T (2020) Characteristics of a Tonian reef rimmed shelf before the onset of Cryogenian: insights from Neoproterozoic Kuniyar Formation, Simla Group, Lesser Himalaya. *Mar Pet Geol*:117

Tinterri R (2011) Combined-flow sedimentary structures and the generic link between sigmoidal and hummocky-cross stratification. *Geo Acta Bologna* 10:1–43

Todd SP (1996) Process Deduction from fluvial sedimentary structures. In: Carling PA, Dawson MR (eds) *Advances in fluvial dynamics and stratigraphy*. Wiley, Chichester, pp 299–350

Tunbridge IP (1981) Sandy high-energy flood sedimentation-some criteria for recognition, with an example from the Devonian of S.W. England. *Sediment Geol* 28(2):79–95

Uroza CA, Steel RJ (2008) A highstand shelf-margin delta system from the Eocene of West Spitsbergen, Norway. *Sediment Geol* 203(3–4):229–245

Vakarelov BK, Ainsworth RB, MacEachern JA (2012) Recognition of wave-dominated, tide-influenced shoreline systems in the rock record: variations from a microtidal shoreline model. *Sediment Geol* 279:23–41

Van Cappelle M, Stukins S, Hampson GJ, Johnson HD (2016) Fluvial to tidal transition in proximal, mixed tide-influenced and wave-influenced deltaic deposits: cretaceous lower Sege Sandstone, Utah, USA. *Sedimentology* 63:1333–1361

Van Yperen AE, Holbrook JM, Poyatos-Moré M, Midtkandal I (2019) Coalesced delta front sheet-like sandstone bodies from highly avulsive distributary channels: the low-accommodation Mesa Rica Sandstone (Dakota Group, New Mexico, USA). *J Sediment Res* 89:654–678

Van Yperen AE, Poyatos-Moré M, Holbrook JM, Midtkandal I (2020) Internal mouth-bar variability and preservation of subordinate coastal processes in low-accommodation proximal deltaic settings (Cretaceous Dakota Group, New Mexico, USA). *Depositional Rec* 6(2):431–458

Visser MJ (1980) Neap-spring cycles reflected in Holocene subtidal large-scale bedform deposits: a preliminary note. *Geology* 8(11):543–546

Walker RG, Plint AG (1992) Wave-and storm-dominated shallow marine system Walker RG, James NP (eds), *Facies models: response to sea level change*. Geol Assoc Canada, St. John's pp. 219-238

Waresak SR (2016) Cyclically-forced hyperpynites of the ancient Colorado River Proximal Prodelta. Loma Linda University Electronic Theses, Dissertations & Projects. 406

Williams GE (1989) Late Precambrian tidal rhythmities in South Australia and the history of the Earth's rotation. *J Geol Soc Lond* 146:97–111

Williams GE (1991) Upper Proterozoic tidal rhythmites, South Australia: sedimentary features, deposition, and implications for the earth's paleorotation. In: Smith DG et al (eds) *Clastic tidal sedimentology*, vol 16. *Mere Can Soc Pet Geol*, pp 161–177

Wilson MEJ (2005) Development of equatorial delta-front patch reefs during the Neogene, Borneo. *J Sediment*

Wilson RD, Schieber J (2014) Muddy prodeltaic hyperpycnites in the Lower Genesee Group of Central New York, USA: implications for mud transport in epicontinental seas. *J Sediment Res* 84(10):866–874

Xue Z, Liu JP, DeMaster D, Nguyen LV, Ta TKO (2010) Late Holocene evolution of the Mekong subaqueous delta, Southern Vietnam. *Mar Geol* 269(1-2):46–60

Young GM, Long DGF (1977) A tide-influenced delta complex in the upper Proterozoic Shaler Group, Victoria Island, Canada. *Can J Earth Sci* 14:2246–2261

Zhang L, Bao Z, Dou L, Zang D, Mao S, Song J (2018) Sedimentary characteristics and pattern of distributary channels in shallow water deltaic red bed succession: A case from the late Cretaceous Yaojia formation, southern Songliao Basin, NE China. *J Pet Sci Eng* 171:1171–1190

Zieliński T, Widera M (2020) Anastomosing-to-meandering transitional river in sedimentary record: a case study from the Neogene of central Poland. *Sediment Geol* 404:105677